RE-ORDER NO. 62-595

A MOISTURE ANALYZER

FOR MARTIAN ATMOSPHERE

This work was performed for the Jet Propulsion Laboratory, California Institute of Technology, sponsored by the National Aeronautics and Space Administration under Contract NAS7-100.

Final Report on

JPL Contract No. 950207

to

California Institute of Technology
Jet Propulsion Laboratory
Pasadena, California

from

Meteorology Research, Inc.
2420 North Lake Avenue
Altadena, California

September 10, 1962

Paul B. MacCready, Jr.

Paul B. MacCready, Jr.
President

MRI62 FR-48

SUMMARY

21042

A four month study and experimental program was undertaken to determine if the MRI phosphorous pentoxide type of moisture meter could be used to measure the expected water vapor in the Martian atmosphere while being lowered to the surface in an instrument package ejected from a space vehicle near this planet. An operating breadboard model of the proposed system was delivered which met or exceeded most of the criteria set forth by JPL for this project.

For the system designed, temperature and sterilization requirements do not appear to impose any severe problems. The space and weight requirements of one pound and 500 cc were surpassed, the model weighing approximately 11 ounces with a volume of approximately 450 cc. Both of these can be readily reduced with additional routine engineering. The overall maximum power requirement of 500 mw can be met, but there would be some advantages if more power were available.

The range of the instrument delivered was shown to be from 3 to several hundred parts per million of water vapor. The present moisture sensor and system is believed to be capable of operation down to levels of 0.5 ppm, but difficulties with providing calibrated moisture sources in this low range prevented this performance being proved conclusively. This problem also prevented establishing the accuracy of the readings at the lowest range, but it is certainly better than ±20% for moisture levels above about 5 ppm. The breadboard was shown to be capable of operating at ambient pressures only as low as 0.5 atmospheres, being limited by the pump supplied. Other similar pumps during the development program operated as low as 0.15 atmospheres and this is believed to be more representative of the capabilities of the present system design.

As a result of the information developed in this program it seems evident that a further modest engineering program would result in the construction of an engineering prototype of an instrument which would satisfy all requirements for the measurement of the moisture in the Martian atmosphere in a simple and reliable manner. Author

INDEX

INTRODUCTION

This final report on JPL Contract No. 950207 describes the work performed by Meteorology Research, Inc. over a four month period directed toward demonstrating the feasibility of adapting the MRI phosphorous pentoxide type of moisture meter to the measurement of the water vapor expected to be encountered in the Martian atmosphere.

The MRI Model 901 Moisture Meter is a portable all purpose unit designed for ground and airborne use, weighing about 20 pounds with self contained batteries for 200 hours of operation. It covers a range of about 10 to 30,000 ppm of water vapor by means of scale switching. It has been operated at altitudes up to 35,000 feet. For the Martian application it must withstand much more rigorous environmental specifications, including sterilization, and must be designed to size, weight and power requirements which would permit its operation on an instrument capsule dropped through the Martian atmosphere from a space vehicle.

The operation of the instrument is based on the electrolysis of water vapor absorbed by a sensor or cell containing phosphorous pentoxide. The current resulting from the electrolysis is a direct linear measure of the amount of water dissociated. A constant voltage is applied across the sensor to cause the electrolysis.

The gas being measured is sampled by drawing a constant mass flow of the gas through the sensor. This is furnished by a pump. A flow sensor is also placed in the line, and the output of the flow sensor controls the pump through a servo amplifier which keeps the mass flow constant over the desired range of ambient pressure and temperature conditions. A temperature compensating means is provided to make the operation of the flow sensor independent of temperature. The general arrangement of this system is shown in Fig. 0.1 on the following page.

The components of the system can be readily broken down into five categories, which are described in detail in the following five sections of this report:

1. The Moisture Sensor
2. The Flowmeter
3. The Pumping System
4. The Readout System
5. The Power Supply

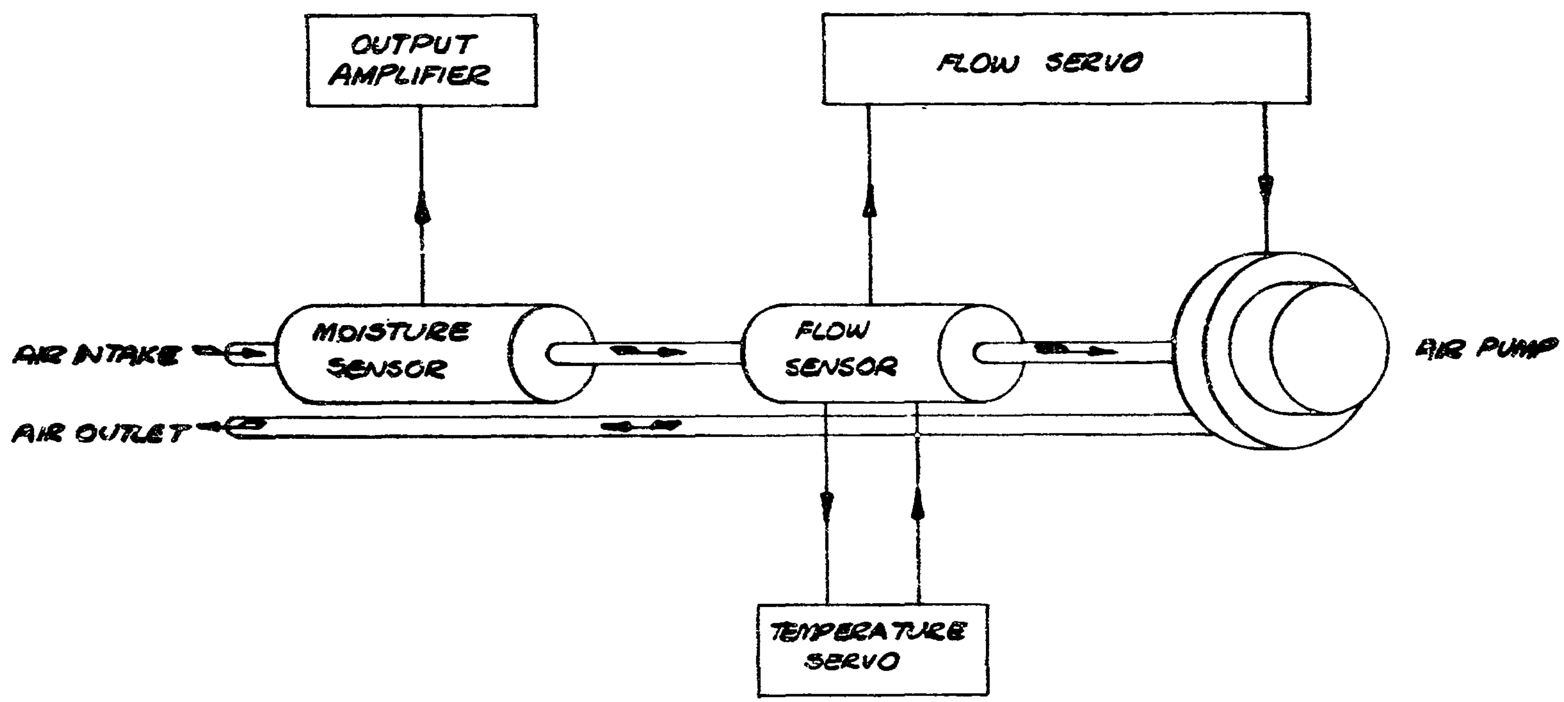

FIG 0.1 - MOISTURE SENSOR SYSTEM

Additional information is presented on the feasibility breadboard instrument delivered as a result of this work, and a discussion is also included on the systems problems and future work which might be undertaken in the further refinement of the instrument. In a final section, the numerical results of the experiments are tabulated.

THE MOISTURE SENSOR

GENERAL DESCRIPTION

The phosphorous pentoxide moisture sensor used in these tests is in theory a chemical moisture trap and electrolytic cell. The trapping agent, P_2O_5, maintains a very low water vapor pressure and equilibrates quite rapidly. The electrolytic cell has two platinum electrodes wound as a very tight double helix on the inside of a small glass tube. The electrolyte, the $P_2O_5 \cdot x\,H_2O$ is introduced as a 10% solution in acetone. When the acetone has evaporated, a potential is applied across the two electrodes to drive off the moisture which is present in the hydrate. The sensor is then prepared to pick up moisture from the atmosphere, electrolyze it, and pass the current necessary to read. Since all the moisture trapped is immediately electrolyzed and the drying agent is itself always dry as a result of the electrolysis, it performs at a continual optimum. The over-all chemistry of this system is:

(1) $P_2O_5 + x\,H_2O \longrightarrow P_2O_5 \cdot x\,H_2O$

(2) $P_2O_5 \cdot x\,H_2O \longrightarrow P_2O_5 + x\,H_2 + \frac{x}{2}\,O_2 + \text{current}$

According to Faraday's law, one gram equivalent of matter (9.01 gms of H_2O) is electrolyzed by one Faraday of current (9.65×10^4 coulombs). Applying this principle to our system we find that at a level of 1 ppm and a flow rate of 10 cc/min we should get a current of 2.23 μ A.

(3) $\text{Gms } H_2O/\text{sec} = \text{amps} \times \frac{9.013}{9.65 \times 10^4} = \mu A \times 9.3399 \times 10^{-11}$

(4) $\text{cc } N_2/\text{sec} = \frac{10}{60}$

(5) $\text{Gms } H_2O/\text{cc } N_2 = \mu A \times 9.3399 \times 10^{-11} \times 6 = \mu A \times 5.6039 \times 10^{-10}$

(6) $\text{Gms } H_2O/\ell N_2 = \mu A \times 5.6039 \times 10^{-10} \times 10^3 = \mu A \times 5.6039 \times 10^{-7}$

(7) $\text{Gms } H_2O/\text{Gm}N_2 = \mu A \times 5.6039 \times 10^{-7} \div 1.25 = \mu A \times 4.4831 \times 10^{-7}$

(8) $\text{Mgms } H_2O/\text{Gm}N_2 = \mu A \times 4.4831 \times 10^{-1} = \mu A \times .44831$

$\therefore$ 1 ppm (by weight) = 2.2306 μ A

This is readily converted to flows of other than 10 cc/min by multiplying by the factor flow/10.

MEASUREMENT TECHNIQUES

For developmental purposes the sensor is mounted mechanically in series with a source of gas of variably controlled moisture and flow rate and a flow sensing device. The cell is electrically in series with a battery and an electrical meter. In actual operation the only real change is the substitution of available atmosphere for the moisture source, and a pump controlled by a flow meter which provides a constant flow.

In most instances readings are taken on a calibrated microammeter with a 5 μ A full scale with shunts to permit readings up to 30 μ A and an amplifier to give readings of .5 μ A full scale. The cell currents are in theory not voltage sensitive. However, response rates are voltage sensitive by factor of 2. Therefore the maximum voltage which will not short out the system is usually the most desirable. Twenty-four volts provides a satisfactory response rate and does not short the system.

One of the major problems in testing this system is determining the exact amount of water being delivered to the sensor per unit mass of carrier gas. It is first necessary to obtain a source of gas with a known moisture content. This is quite difficult in the region of interest, namely, below 10 parts per million. We were unable to find any commercial sources of such gas, other than nitrogen guaranteed to be "less than 9 ppm" or "less than 5 ppm" for example. There are no moisture measuring devices which will function in this region as a standard, so it is necessary to determine the moisture content by indirect means.

A reference level of essentially zero moisture can be established by a series of moisture traps. A P_2O_5 drying trap is very efficient, but all that can be established is that the air passing through a fresh trap contains less than 0.1 ppm of moisture. Exactly how much less will depend upon the flow rate, trap size, and the quantity of moisture previously trapped. If the trap is made like the sensor, with an electrolytic system, essentially zero moisture can be obtained.

This technique has two serious drawbacks. First, it only permits "zero" moisture and second, it introduces background noise. One of the end products of the electrolytic reaction (equation no. 2) is hydrogen. These moisture cells appear to be somewhat sensitive to hydrogen as shown below.

(9) $P_2O_5 + x\,H_2 \longrightarrow x\,H_2O$ + some compound of P

(10) $P_2O_5 + x\,H_2O \longrightarrow P_2O_5 \cdot x\,H_2O$

In order to eliminate this difficulty, a P_2O_5 sensor can be used as a preliminary system dryer and then a liquid nitrogen cold trap used to insure a zero moisture base line. After establishing the base line, progressively warmer traps are substituted to control the moisture content over a broad range. Such a system is shown in Fig. 1.1 .

After establishing with great care what is believed to be a certain moisture level by this method, it might be supposed that checking the calibration or response of a moisture cell would be easy. Unfortunately, this turned out to be the most difficult part. The source of gas of a computed moisture content must somehow be connected to the sensor being tested. There is a wealth of experience and information available concerning techniques for handling zero moisture gasses, particularly in high vacuum systems. One makes a tight system and then bakes all the moisture out of the walls. Barring leaks, there is no further trouble. Our problem, however, turned out to be vastly more difficult, and was the major item in slowing the progress of the development.

We needed a system in which the moisture content could be varied and controlled up to a level of about 10 ppm. We found very little information about this problem in the literature, and some of the reports of certain "satisfactory" techniques we found to be inoperable and erroneous. No matter what scheme we used to connect the gas source to the sensor we were plagued with a host of moisture sinks and sources in the connecting means. These are of no consequence at high moisture levels, and at zero levels their effect can be eliminated by heating. They can give errors of several hundred per cent at moisture levels in the 10 to 0.01 ppm range, however. These sinks and sources were characteristic of the tubing, seals, and couplings which were necessary to connect the sensor to the gas source.

Following the recommendation of experimenters who claimed to have used them satisfactorily at these moisture levels, we employed teflon and glass tubing and a silicon elastomer was used to seal all the connections in our early system. Much time was lost before we were able to establish that the elastomer, and apparently most similar elastomers, contained very large quantities of water. This would be given off into the system at irregular intervals in amounts which would completely mask the desired observations.

In addition to the problems in the connecting tubing, it is necessary to control the environment of the sensor itself as its construction is not positively airtight. In our early teflon systems we tried encasing the sensor in teflon as diagrammed in Fig. 1.2 . After this proved unsatisfactory, the sensor was mounted as in Fig. 1.3 which provided a gas environment for the sensor which was identical to the gas passing through the

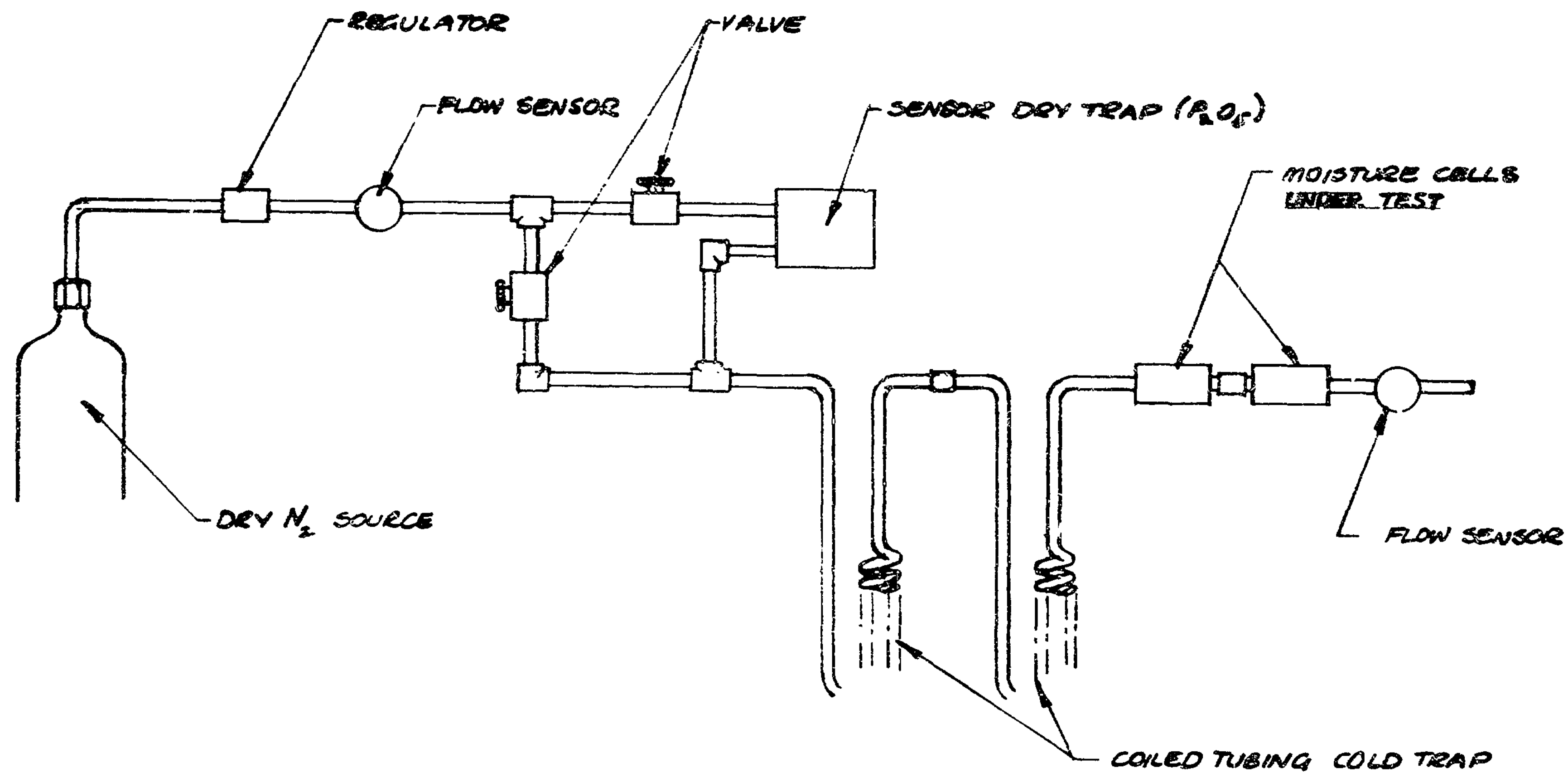

NOTE: ALL PARTS DOWSTREAM FROM FIRST FLOW SENSOR ARE STAINLESS STEEL

FIG 1.1 - FINAL TEST APPARATUS

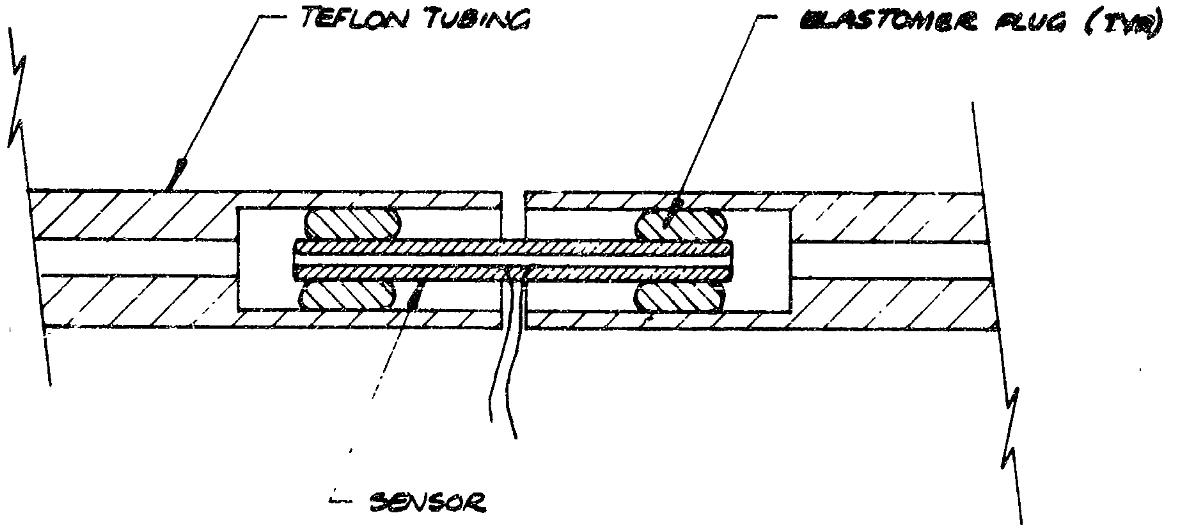
TEFLON TUBING
ELASTOMER PLUG (TYP)
SENSOR

FIG. 1.2

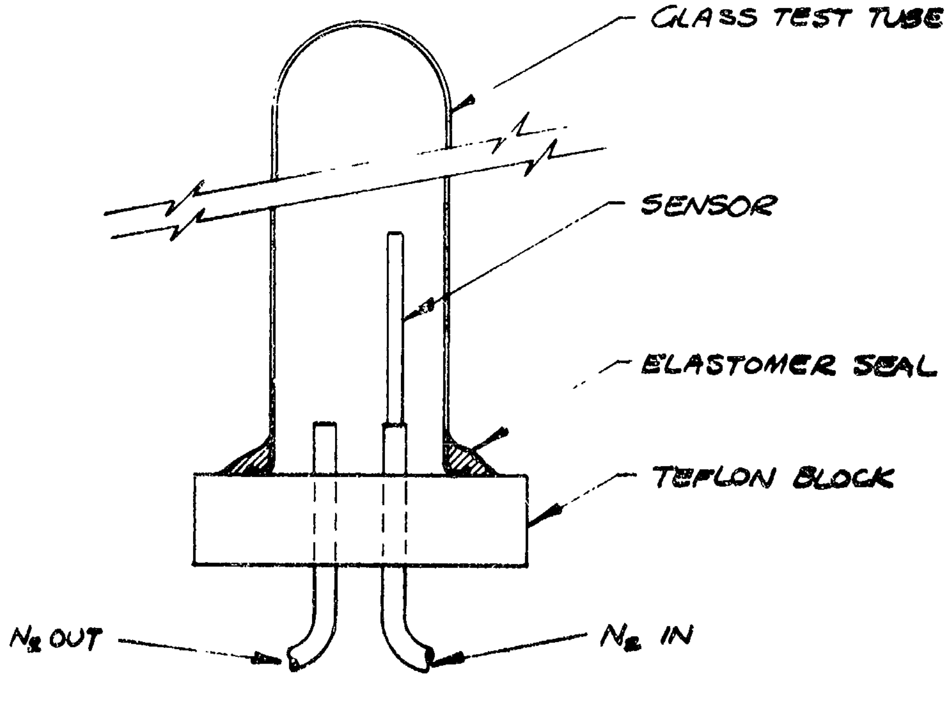
GLASS TEST TUBE
SENSOR
ELASTOMER SEAL
TEFLON BLOCK
N_2 OUT
N_2 IN

FIG. 1.3

sensor. This was done by having the environment be the discharge gas from the sensor.

We finally went over entirely to stainless steel tubing with ferruled joints. This is by no means perfect, but is the best we have been able to find to date. Its use enabled us to get satisfactory calibrations of the sensors down to 3 ppm. Lower moisture levels were still giving erratic results, despite the most careful cleaning and handling of the stainless tubing and connections.

With our stainless steel system we have potted the sensor in a hard setting epoxy. The working cell is in a metal case with a high temperature epoxy filler. It weighs .25 ounces and has a volume of .1 cu. inch and is shown in Fig. 1.4.

OBSERVATIONS

All of the early calibration system setups proved to be useless except as clues to improving design of the system itself. They provide very little meaningful data about the sensors. Some of the errors discussed in the next section are based on these early observations but they were systems which do not supply a fine control over a very low moisture level.

Using the teflon and silastic system it was possible to obtain milimicro-ampere readings. Baking the sensor for several hours and then cooling gave a reading which implied a 2 ppb moisture content. However, turning the heat lamp off for a few hours resulted equilibration to a level of 30 or 40 ppm. Removal of silastic eliminated this problem.

For high level readings of 100 ppm and up, the results of sensor output versus moisture are quite linear. Below this, as reported by other investigators, the silastic which was used as a sealing agent yields water at a sufficient rate to maintain readings several fold higher than the moisture which could pass the cold trap would produce.

Theoretically a change in flow should produce a parallel change in microamp output reading from the sensor, as the moisture content being introduced to the sensor per unit time should be a function of the flow rate as well as the moisture content of the carrier gas. In actual observation, however, when the system has been taken to a relatively dry state, what occurs is the reverse; an increase of flow will produce a reduction in current flow. This is a temporary reduction and readings will rise back to normal background. However this causes some doubt as to whether the readings are actually due to moisture being carried by the gas. It would certainly indicate that they are not due to moisture being carried through the moisture traps by gas but that they are probably caused by moisture

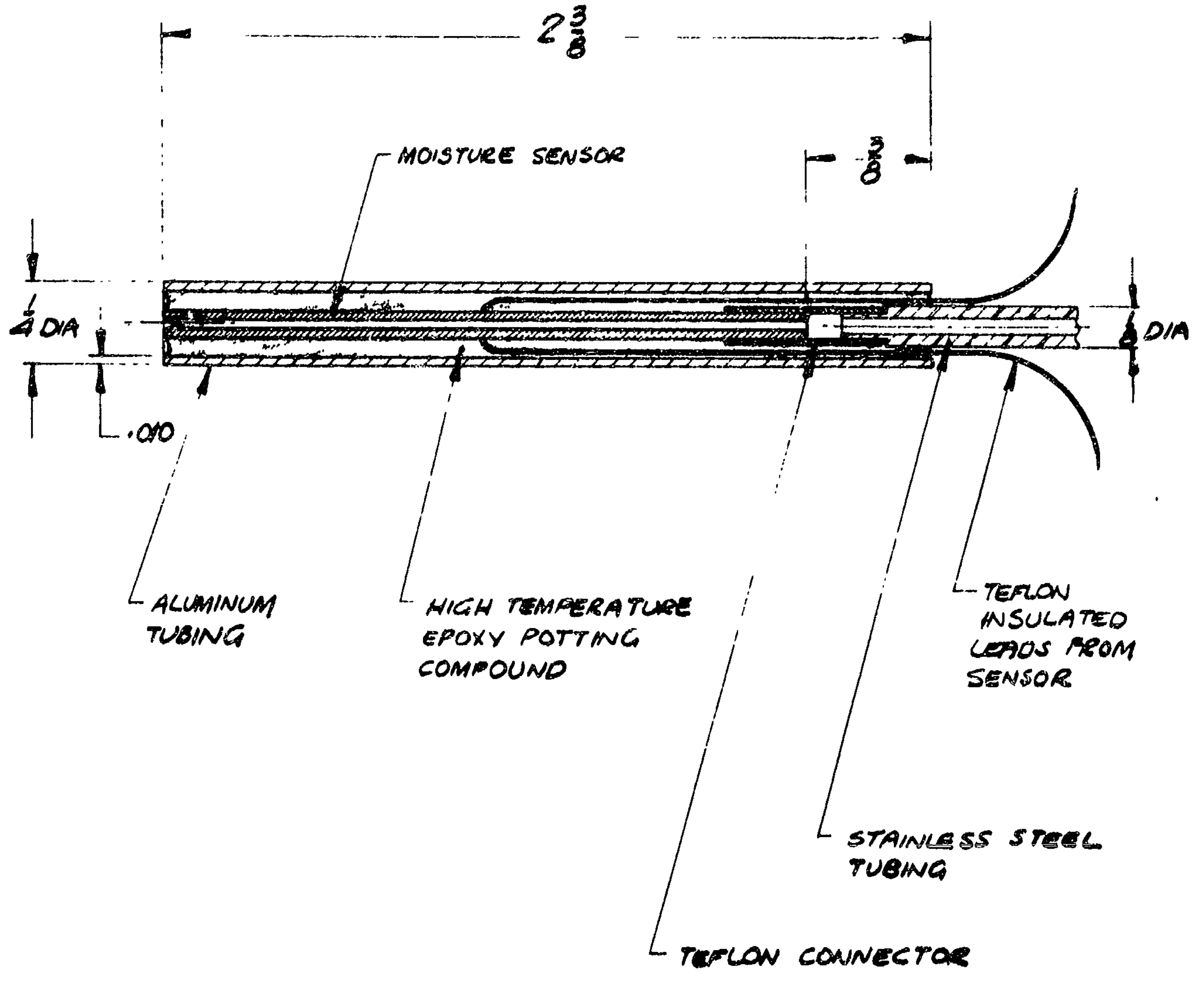

FIG. 1.4 FINAL SENSOR CONFIGURATION

being released from a moisture source some place in the system between the trap and the sensor itself.

In an attempt to eliminate the above mentioned irregularities the stainless steel system was put together. On the first run using the system, the system itself was dried with high-purity dry nitrogen gas passed through a 30-inch P_2O_5 sensor to remove the last few parts per million. After approximately 60 hours of drying, the cold trap was filled with liquid nitrogen and the sensor by-passed. This permitted a thin layer of ice to accumulate inside the coil while still drying the sensor and all of the stainless steel located between the sensor and the coil. This ice layer insures the presence of moisture when the system is allowed to warm. After approximately 90 hours at 40 cc/min the current was approximately 3 microamps. Therefore the apparent indicated moisture was approximately .35 ppm.

This was considered background, as it held for several hours and then started to rise slightly but leveled and held again. Rapidly removing the liquid nitrogen and replacing it with ethanol cooled to -111.6°C started the warmup. After 11.5 hours the temperature was -75°C and the moisture content should have been greater than 1 ppm. The reading was still approximately 3 microamps or .35 ppm. The cold trap coil was then removed from the cold bath and allowed to warm rapidly to room temperature. This produced a reading which rapidly rose to levels above 500 mgm/kgm.

Several changes were made in the system at this point in an attempt to eliminate this effect. The first was based on the assumption that the 90 volt potential employed might be causing the system to equilibrate with some hydrate of the P_2O_5 present which was not as efficient a dehydrating agent as some of the others. To correct this, the voltage was changed to 22.5 volts on the assumption that this would probably cause equilibration with a different hydrate. Since there was some possibility that the gas coming out of the cold trap might still be cold when it reached the sensor and possibly even be freezing the sensor, a second coil was introduced which was kept at ambient temperatures. This coil appears in the diagram of the stainless steel system, however it was not in the system originally.

A recorder plotting current output from the sensor was added to the system at this point and the drying process was recorded. It is a fairly smooth curve behaving much as could be expected. However, in this instance when we shunted the first sensor being used as a drying trap we did not have the coil previously set in liquid nitrogen. Contrary to what might be expected this did not produce a rapid increase in the readings. When there was no increase we allowed this system to run and it took 5.5 hours before the moisture in the system produced any effect on the sensor.

We assumed that this was due to the shunted trap still having some effect through diffusion. For this reason, when the system was dried for the next run, after inserting the coil in liquid nitrogen and before allowing the warmup to start, the sensor being used as a drying trap was completely removed from the system and the system closed rather than simply shunted.

This system had a background reading of 3.2 microamps even though the cold bath temperature at the start was approximately -119°C. The background readings not only did not come up with increasing temperature but they continued to fall an additional .04 microamps. When the temperature had risen to -50°C which should have been passing 29 ppm through the cold trap, the readings suddenly started to come up comparatively rapidly and rose continually to 10 ppm at which time the experiment was stopped.

It is possible to explain the above result by assuming that the apparent background of 3 microamps was not actually a dry system background reading, but that this was the reading produced by the moisture being driven off from some hydrated form of P_2O_5, but there are several hydrates of phosphorous pentoxide - phosphoric acid, pyrophosphoric acid, metaphosphoric acid - the water contents of which are indicated as follows:

$$2H_3PO_4 = P_2O_5 \cdot 3H_2O$$

$$H_4P_2O_7 = P_2O_5 \cdot 2H_2O$$

$$2HPO_3 = P_2O_5 \cdot H_2O$$

It would be possible to electrolytically remove the water from these hydrates according to the following reaction pattern:

$$H_3PO_4 \text{ (in solution)} \xrightarrow{V} H_2PO_4 \cdot \tfrac{1}{2} H_2O$$

$$2H_3PO_4 \cdot \tfrac{1}{2} H_2O \xrightarrow{V} 2H_3PO_4 + H_2O$$

$$2H_3PO_4 \xrightarrow{V} H_4P_2O_7 + H_2O$$

$$H_4P_2O_7 \xrightarrow{V} 2HPO_3 + H_2O$$

$$2HPO_3 \xrightarrow{V} P_2O_5 + H_2O$$

If this be so, then we probably have a series of such apparent background readings, each one indicating the potential difference between the hydrate being formed and the hydrate being broken down. It would not be unreasonable to assume that such dehydration process of removal of water of crystallization in this case would take in excess of 15,000 hours as indicated by the following calculations:

$\sim .1$ mgm H_3PO_4 in coating

Mol. wt. $H_3PO_4 \sim 100$

$.1$ mgm $H_3PO_4 \sim 10^{-6}$ moles H_3PO_4

10^{-6} moles $= 6 \times 10^{7}$ molecules

3μ A $\sim 10^{10}$ molecules/sec

$$\frac{6 \times 10^{17}}{10^{10}} = 6 \times 10^{7} \text{ sec}$$

$$= 1.5 \times 10^{4} \text{ hr.}$$

The addition of water in the manner in which we have done in our previous setups would then not be able to cause a significant increase in rate of reaction but would rather for quite some time be electrolyzed only at the same rate as its potential difference would permit, the excess of water beyond this being taken in to reverse the process and cause hydration to occur.

It is possible however to greatly increase this rate of removal of water of crystallization. Most chemical reactions will approximately double their rate for each 10°C increase in the temperature of the system. Also their reaction rate will vary approximately proportionately to the driving force of the reaction. Therefore, by applying heat to the system and boosting the voltage it would be possible to increase this rate. An increase of approximately 110°C would cause a rate increase of approximately 2,000 fold and an increase in the voltage of four fold would bring this up to approximately an 8,000 fold increase in reaction rate. At this rate it would take somewhat in excess of 50 hours to dry the system. The reason for the uncertainty of how long is primarily that as the system gets drier the reaction will slow down.

It is possible that a sensor design modification could shorten this time considerably. The present sensor has the electrodes wound inside the glass which produces large P_2O_5 pockets that have little or no potential for electrolysis. If a plating technique could be employed these spaces would be eliminated and the P_2O_5 present might be reduced to 5 to 10% of that needed currently. This would shorten the drying time an additional 90 to 95%.

A further improvement might be to shape the inside of the sensor in the form of a cone. This would give a swirl to the air passing through. The effect would be to effectively increase the length of the cell without actually increasing its length or quantity of P_2O_5, but this would be a difficult mechanical construction and other means should be tried first.

The most obvious technique would be to reduce the thickness of the P_2O_5 coating in the standard sensor. This was subsequently done, and the results of the tests with such a configuration seemed to indicate that moisture sources and sinks in the connecting tubing were still playing a major part in the erratic behavior at very low moisture levels.

ERRORS AND LIMITATIONS

This system has several inherent sources of error which can be grouped in three major categories: spurious moisture input, mass flow control, and measurement of electrolytic current. Two sources of error in moisture input for all test systems are internal sinks and sources. Internal sources are effectively eliminated by continuously pumping dry air through the system until it is satisfactorily dehydrated and no further changes in current occur. With the system modified to remove the background reading, this would be when a smooth continuous zero occurs. In a continuous flow system, moisture sinks are not a major problem in terms of magnitude since they will saturate, but they do interfere with response rates when flow or moisture changes. This will not be true if there is a large P_2O_5 sink, as its moisture capacity would cause it to take up all of the water for quite some time.

For those test systems in which moisture is regulated continuously by a cold trap from a base line to a high level there is the additional error due to temperature measurement of the bath. This is reduced to a minimum by having a copper-constantan thermocouple attached directly to the cold trap coil. Such a system gives a .018 millivolt change per °C approximately and is therefore quite accurately measurable to within at least .1°. The thermal conductivity of stainless steel is sufficiently high that there is thermal equilibration of the air flow to within ±1°. We can, therefore, know our moisture input to approximately ±5% at any level under steady state conditions.

With regard to the measurement of mass flow, we are using the same thermistor flow meter which has been designed for the operational system. This meter is discussed elsewhere in this report, however for the purposes of this section, it is definitely not limiting.

A 5 microamp full-scale ammeter was used for current measurement. It had a 10 times amplifier and was scaled to permit 3% readings at all ranges from 0.01 microamps to 5,000 microamps.

With reference to the moisture sensor itself, it has previously been noted that a dried and baked-out cell has a current output equivalent to two parts per billion. This indicates that the inherent lowest moisture level that can be detected by this technique is very small indeed, and probably limited by the ohmic resistance of the cell. The behavior of the cells during our test runs seems to indicate that with the relatively thick P_2O_5 coatings we were using there could be a low-level masking effect caused by interchanging of moisture between parts of the P_2O_5 in the cell which are not subject to the electrolyzing voltage, and those which are between the wires where they are subject to electrolysis. We believe engineering improvements on the present cells would permit moisture levels of 0.5 ppm to be measured, with levels of 0.01 ppm becoming possible after considerable design improvement in the construction of the cell internal parts. We believe it likely that our sensors in their present form are capable of much lower readings than the 3 ppm we were able to obtain in our calibration runs (Fig. 1.5), but it was not possible to determine this because of the difficulties with the moisture standard which were described above. Extensive tests of sensors with various coating thicknesses to determine the effect of this variable on sensitivity, range, time constant, output, etc., had been planned, but it was not possible to carry them out in the time available, because it was necessary to spend the time on moisture standard experimentation.

A question has been raised concerning the possible evaporation of the P_2O_5 if the cell is exposed to the high vacuum of outer space for a long period of time, such as during transit to Mars. It has not yet been established if this would occur. However it would not be a serious problem since it can be checked by terrestrial experiments in a vacuum chamber, and if no other solution is found the cell can readily be sealed during its flight.

In summary, the P_2O_5 moisture sensing cell in its present form appears to be capable of effectively measuring the moisture in the expected Martian atmosphere over a range of at least three to several hundred parts per million, and is probably capable of measuring much smaller values. The expected ambient conditions, and presence of other gases will not seriously affect its operation.

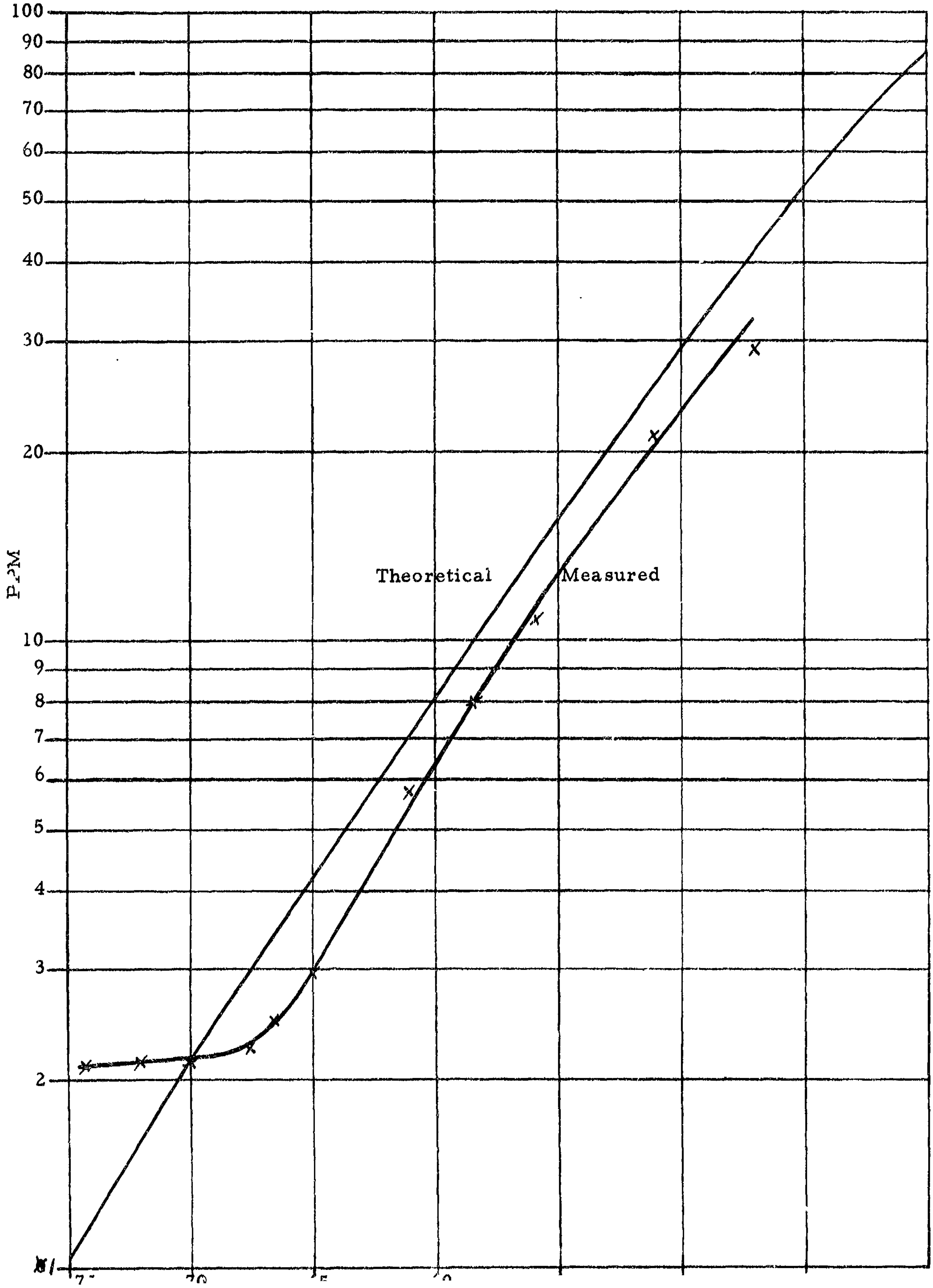

100
90
80
70
60
50
40
30
20
10
9
8
7
6
5
4
3
2
P_2M
Theoretical
Measured

THE FLOWMETER SYSTEM

GENERAL

The moisture absorbed by the sensor will be a function of the mass flow of gas through the sensor, and this quantity must be known if the sensor electrical output is to have any absolute significance. If the mass flow varies, it must be measured simultaneously with the sensor output, or must be capable of determination by indirect means. Measurement or computation of this variable is avoided, however, if the flow is kept constant at some known value. This is the scheme used in the MRI moisture meter on which this development is based.

A heated thermistor bead placed in the gas stream will be cooled by the gas, and when placed in a Wheatstone bridge arrangement will give a signal output proportional to mass flow. The bridge output is amplified in an amplifier and through conventional servo techniques drives a pump which creates and thus holds a constant mass flow. The pump system and its servo are described in Section 3.

The simple system described above operates satisfactorily under normal ambient conditions, but when exposed to extremely high or low temperatures there is an error caused by the ambient temperature changing the resistance of the thermistor. This error can be eliminated by a thermostatically controlled heater keeping the flowmeter at a constant temperature (above ambient), or by use of a compensating thermistor whose temperature is controlled. This latter system has certain advantages and has recently been applied to the conventional MRI moisture meter, and has been used on the Martian unit as well. It is described in detail in the following paragraphs. A third system of temperature compensation has been proposed, but not tested, which utilizes an alternating current to heat the thermistor. This would be more economical of power than the two systems outlined above, and should be tested in the future for possible application on this project.

Temperature Compensated Flow Sensor:

Two thermistor beads are used. The "active" bead is placed next to a constriction in the gas flow to be measured so that the gas strikes it and cools it. The "compensating" bead in the cavity filled with the same gas is located so no flow cools it. Both beads are mounted in a block through which the flow passes as shown in Fig. 2.1. They are arranged in a Wheatstone bridge in the usual way so that the electrical output from the bridge varies with flow rate. This output usually also varies with ambient temperature. To prevent this, the block is heated by a transistor held in good thermal contact with it, and the current flowing through this transistor is made to vary directly with the voltage across the compensating bead (Fig. 2.2).

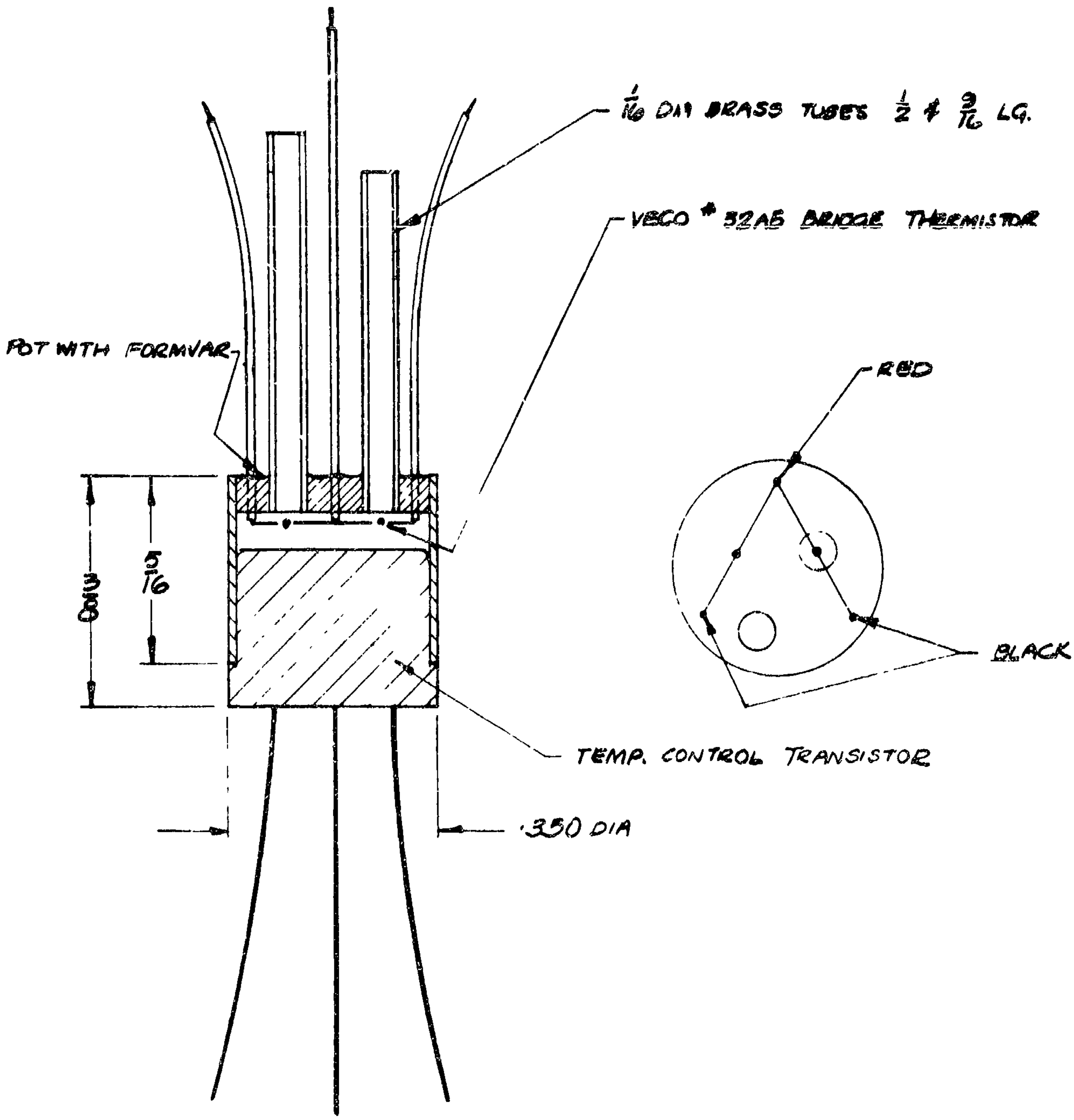

FIG 2.1 - FLOW SENSOR

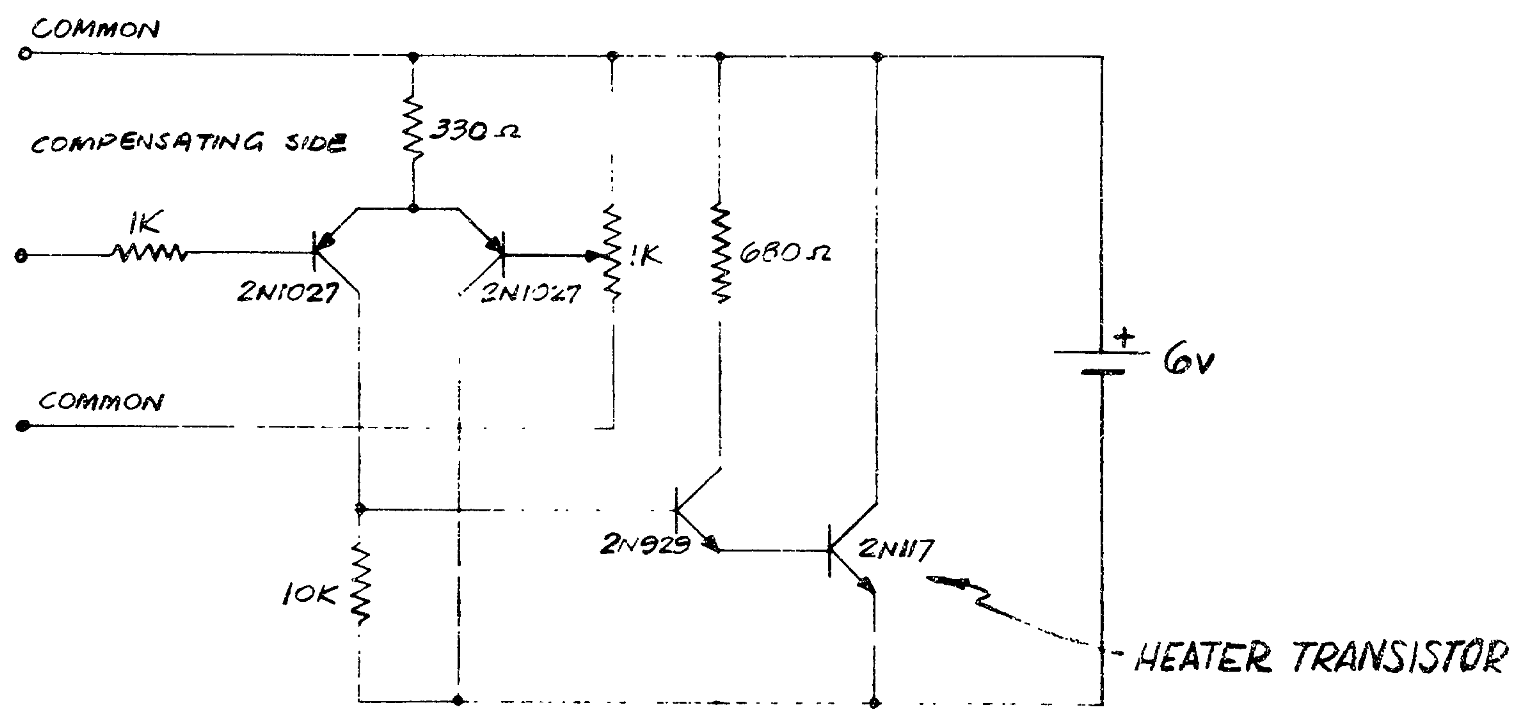

FIG 2.2 - TEMPERATURE CONTROL FLOW SENSOR CIRCUIT

This forms a negative feedback loop in which (for a given gas composition) the compensating bead resistance--and hence temperature--remain nearly constant in spite of wide ambient temperature changes. The circuit can be adjusted to maintain the compensating bead temperature at any chosen value--this would be chosen to maintain the block rather above the highest ambient temperature expected.

The advantage of controlling the block (and gas) temperature with respect to the compensating thermistor, rather than keeping it constant as with a thermostat, is that the temperature of both beads is maintained constant in face of changing gas conductivity and specific heat as well as changing ambient temperature. This causes the mass flow to vary to a predictable and fairly small extent with conductivity and specific heat. With thermostat type control the mass flow would vary to a greater extent, and this variation would also depend on the temperature/resistance characteristics of the individual thermistors used. The reasons for this are given below.

W_a, W_c	=	power dissipated in "active" and in "compensating" beads
$s = C_p$	=	gas specific heat at constant pressure
k	=	gas thermal conductivity
ρ	=	gas density
a	=	bead radius
V	=	velocity of gas past bead
m	=	mass flow of gas
A	=	area of gas channel near "active" bead
T_a, T_c	=	temperature of "active" and "compensating" beads
t	=	temperature of gas near beads, (= block temperature)

King's Law can be applied to the power dissipation of the active bead if it is assumed that the bead approximates to a cylinder of radius a and length $2a$:

$$W_a = 2a\left(k + 2\sqrt{k\,s\,a\,\rho V}\right)(T_a - t)$$

and $W_c = 4\pi k a\ (T_c - t)$

ignoring convection in both expressions.

$$\therefore\ W_a = 2a\left(k + 2\sqrt{ks\frac{a}{A}m}\right)(T\ - t)$$

In the moisture meter, the sensor is operated in a servo loop with a pump, which varies on such that $T_c = T_a$ (i.e., the thermistor bridge balances at all times). So we have by combining the expressions for W_a and W_c,

$$\frac{W_a}{2a\left(k + 2\sqrt{ks\,a/A'}\;m\right)} = \frac{W_c}{4\pi k a}$$

$$\text{or} \quad m = \frac{A}{a}\left(\pi\frac{W_a}{W_c} - \frac{1}{2}\right)^2 \cdot \frac{k}{s}$$

This relation applies whether or not the sensor is temperature controlled. If it is not, variation in ambient temperature has a large effect on the ratio W_a / W_c as well as a smaller one on the gas "constants" s and k. If the block temperature is simply fixed, by a thermostat-heated arrangement, effects of change in ambient temperature are of course eliminated. However, changes in s and k due to variation in the chemical composition of the gas will not only affect the ratio k/s, but also change the temperature of the beads with the result that W_a and W_c will both vary according to the temperature/resistance characteristics of the beads. The consequent variation in W_a / W_c, and hence m, is large.

Now if heater feedback is applied to the block such that T_c, rather than t, is kept constant, both W_a and W_c remain constant--in spite of changes in k and s, as well as in ambient temperature. We can now write for any gas or mixture of gases, at any temperature within the controlling range of the feedback loop

$$m = (\text{constant}) \times \frac{k}{s}.$$

The ratio k/s varies much less than either k or s individually, among common gases not too near their boiling point.

<u>Table of Specific Heat (at Constant Pressure) and Conductivity For a Few Gases</u>

	AIR	N_2	O_2	H_2	He	CO_2	NH_3
$k \times 10^{+4}$	.57	.52	.56	3.63	3.4	.31	.45
$s\ (= C_p)$	.24	.25	.22	3.38	1.25	.19	.52
$ks \times 10^{+4}$	.14	.13	.12	12.3	4.2	.06	.23
$k/s \times 10^{+4}$	2.4	2.1	2.5	1.08	2.7	1.63	.88

Flow System Characteristics:

With the temperature compensating system in use, it will be noted that the flow system includes two servos driven from the thermistor bridge circuit, one controlling the flow and the other the temperature compensation. Their detailed circuits are shown in Section 6, which describes the breadboard. The flow servo portion of the flow system is very similar to the temperature servo of the system. The flow sensor's active bead, as mentioned earlier, is mounted in the path of the moving air and is cooled by this flow of air. The bridge is so adjusted that when the desired rate of flow is established the bridge is in balance. The servo amplifier receives the balance signal and controls the pumping rate as described in the pump section.

The power requirement for the flow sensor is about 80 milliwatts for the flow function. The heater requires about 300 milliwatts for about 10 to 20 seconds for warmup and then consumes about 110 milliwatts with the flow sensor uninsulated. This, of course, varies as a function of ambient temperature and represents the worst expected conditions. Ordinary foam insulation can readily reduce the steady state heater current by an order of magnitude. The initial warmup power can be spread out over a longer or shorter period than the 10 to 20 seconds provided, with of course approximately the same total electrical energy consumed.

The flow sensor weighs 0.1 ounces including the heater transistor. It uses a volume of .15 cu. in. The weights and volumes of the servo systems are discussed under the pump section.

The flow sensor can sense a flow change of less than .05 cc per minute for flows between 1 and 40 cc per minute.

Running three flow sensors continuously for three months there have been no failures. More meaningful reliability statistics would require greater calendar time; however, two other flow sensors using the same components, less the heater transistor, have been used for three years without any failure. Meteorology Research, Inc. has never had a failure of any flow sensor which was being used properly which had run past an initial break-in period of 48 hours.

Since the operation of the flow sensor depends upon the cooling of a heated element by the gas flowing past it, an investigation was made to determine if the lowest gas density expected to be encountered in the Martian application would still be sufficient to permit this mode of operation. Tests showed that the flow sensor could be used down to pressures of 0.01 atmospheres, so this would not be a problem in this application. At somewhat lower pressures, in the micron and sub-micron pressure range, the heated thermistor starts acting similarly to a Pirani or thermocouple vacuum gauge, and then is affected by the pressure.

The flow sensor as provided fulfills the requirements for the proposed Mars operations. The alternating current type, which has been studied independently by MRI, shows excellent promise of providing a similar flow sensor function while permitting immediate warmup and with less continuous heater power.

THE PUMPING SYSTEM

GENERAL DISCUSSION

The pump development program was initiated by investigating all existing low capacity pumps in the range 0 to 200 cc/min at standard temperature and pressure with a head pressure of at least one inch of water. All pumps investigated (piston, gear, vane, diaphragm, turbine and peristaltic) failed in regard to one or more of the following general requirements; namely: weight, size, operating temperature limits, vibration and input power. By modifying designs and using special materials, it is quite possible that one or two available pump systems could be utilized, except that the input power requirement could not be met regardless of the extent of modification. The only pump system which exhibited promise of meeting all requirements, including low input power, was a vibrating diaphragm type such as are commonly employed in aquarium aerating systems. No such aquarium pumps are in existence which would meet the specifications, so it was necessary to undertake the development of a new pump utilizing the basic principles employed in aquarium diaphragm pumps. It is of interest to note that this type of pump is extremely reliable and extremely long lived, i.e., it is quite common for such inexpensive pumps to operate continuously 24 hours a day for a year or more without failure.

Basically this pump is nothing more than a diaphragm stretched across a small chamber fitted with two small flapper valves to control the flow, as shown in Fig. 3.1. This method of moving small quantities of gasses at low pressures is inherently efficient since frictional losses in the piston diaphragm and flapper valve system can be made small and proper design of the intake and exhaust ports and ducting will reduce air drag and turbulent losses to an insignificant level. The principal energy loss will occur in the drive system, consisting of the transistor circuitry, electro-mechanical diaphragm drive, and coupling between the driver and the diaphragm.

The development program was divided into two sections, one pertaining to the driver and the associated equipment, and one pertaining to the diaphragm and valve system.

DIAPHRAGM AND VALVE SYSTEM

An extensive search was made for diaphragm and valve material which would satisfy the following requirements:

1. High strength in the thickness range 1/2 to 2 mils
2. High strength at low and high temperatures
3. Low coefficients of thermal expansion
4. Light weight
5. Low shrinkage with time, temperature and humidity changes

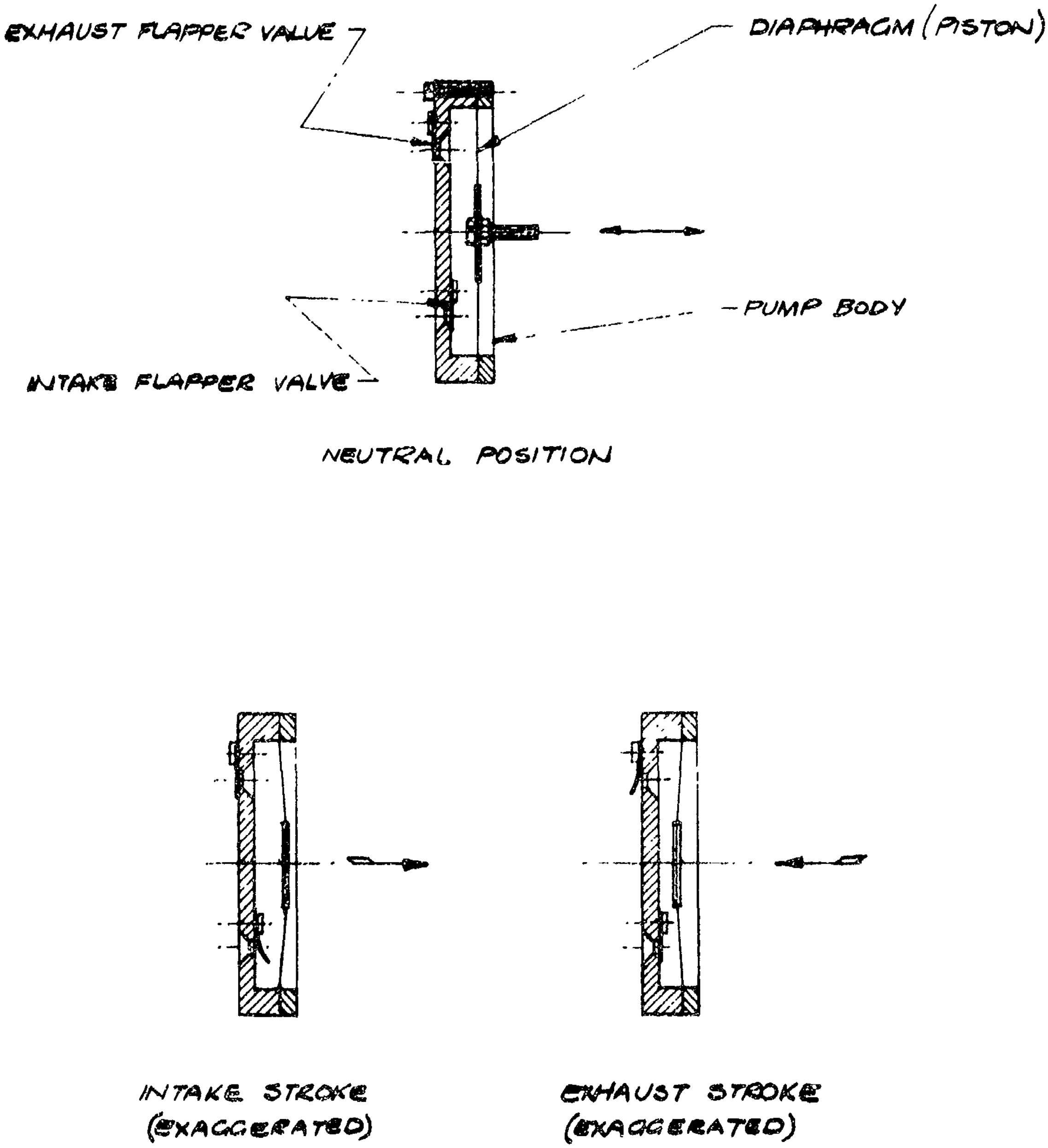

FIG 3.1 - DIAPHRAGM PUMP OPERATING CYCLE

6. Chemically inert
7. Negligible water absorption
8. High flexural strength

Three materials were found which satisfied most of these requirements; silicone rubber, teflon, and mylar. Silicone rubber was eliminated because it could not be obtained in thicknesses less than approximately 0.030 inch. Teflon was eliminated because it had negligible tear and flexural strength in the form of thin films less than 5 mils thickness. Dupont Mylar Polyester Film was selected because it met or exceeded every requirement. It can be obtained in some five standard thicknesses in the range 1/4 mil to 2 mils. Some of its properties are indicated below:

Tensile Strength: 20,000 psi

Break Elongation: 100%

Bursting Strength: 45 lbs per mil

Tear Strength: 15 grams per mil

Folding Endurance: >100,000 (180° crease type folds)

Melting Point: 250° to 265° C

Service Temperature: -60° to 150° C

Coefficient of Thermal Expansion: 15×10^{-6} in/in/°F

Shrinkage: 2 to 3 per cent (30 min at 150°C

Moisture Absorption: Less than 0.5% (total emersion)

Hygroscopic Coefficient Expansion: 11×10^{-6} in/in/% RH

Fungus Resistance: Inert

Acid and Solvent Resistance: Excellent

Since it is critical to the performance of the pump that the flapper valves and diaphragm do not change shape at high or low temperatures, numerous samples in the thickness range 1/4 to 2 mils were tested at -5°F and 310°F (-20°C and 154°C) for several hours. Such tests would in no way change the physical properties of material itself but internal stresses and shrinkage could cause the sample to change shape; e.g. curl, etc. Samples were cut in the form of squares (1 in. x 1 in.), rectangles (1 in. x 6 in.), and circles (1-1/2 in. o.d.) and subjected to the temperature extremes indicated. Plain

Mylar did not curl or deform in any manner except for an initial irreversible shrinkage of 2 - 3% at the high temperature as specified by the manufacturer. The same results were obtained when the samples were placed on a flat plate or clamped between two flat plates. Extreme curling was observed for Mylar samples vacuum plated with thin coatings of aluminum. The conclusions drawn from these series of experiments indicate that Mylar is ideally suited to this application and that it is only necessary to use pure Mylar film which has been pre-shrunk by baking at a temperature of 300°F for approximately one hour.

An experimental pump powered by a solenoid was fabricated to measure pumping speed and efficiency as a function of various Mylar diaphragm and flapper valve thicknesses. The diaphragm thickness was varied over the range 1.5 mils to 3 mils and the valve thickness 0.5 mils to 1.0 mils. No measurable performance change was observed as a function of valve thickness and only a slight change was observed for the various diaphragm thicknesses as shown in Fig. 3.2.

Various flapper valve support methods were tested as shown in Fig. 3.3. Configuration (A) provided maximum support for the valve with regard to environmental vibrations and acceleration loads; however, such an arrangement restricts the air flow thus reducing the pumping speed. In addition, temperature changes alter the tension of the valve due to the expansion and contraction of the Mylar ribbon which would then make the pumping speed sensitive to temperature. Configuration (C) provides low resistance in the open position and is insensitive to temperature changes; and, therefore, is used in the final design.

The Mylar manufacturer informed us that we could expect essentially unlimited life from such diaphragms and valves due to the low stresses involved and limited operating temperatures. Bending of the flapper valves could cause eventual failure; however, Dupont has obtained more than 100,000, 180° crease type folds before failure. It is estimated that greater than 10^8 small angle flexures can be sustained by Mylar before fatigue failures would occur. Several 0.5 to 2 mil Mylar valve and diaphragm assemblies have been operated continuously for periods up to 20 hours at a drive frequency of 250 cps without measurable change in pumping speed. Many hours of handling, modifying and adjusting Mylar diaphragms and valves during the various development and testing activities have shown them to be extremely rugged and durable. Reasonable care in manufacture and assembly to eliminate holes, cuts, or creases will produce a pump diaphragm and valve system with essentially unlimited life when subjected to the specified environment.

Upon selection of the diaphragm and valve material and thickness a prototype pump was fabricated to determine experimentally the optimum

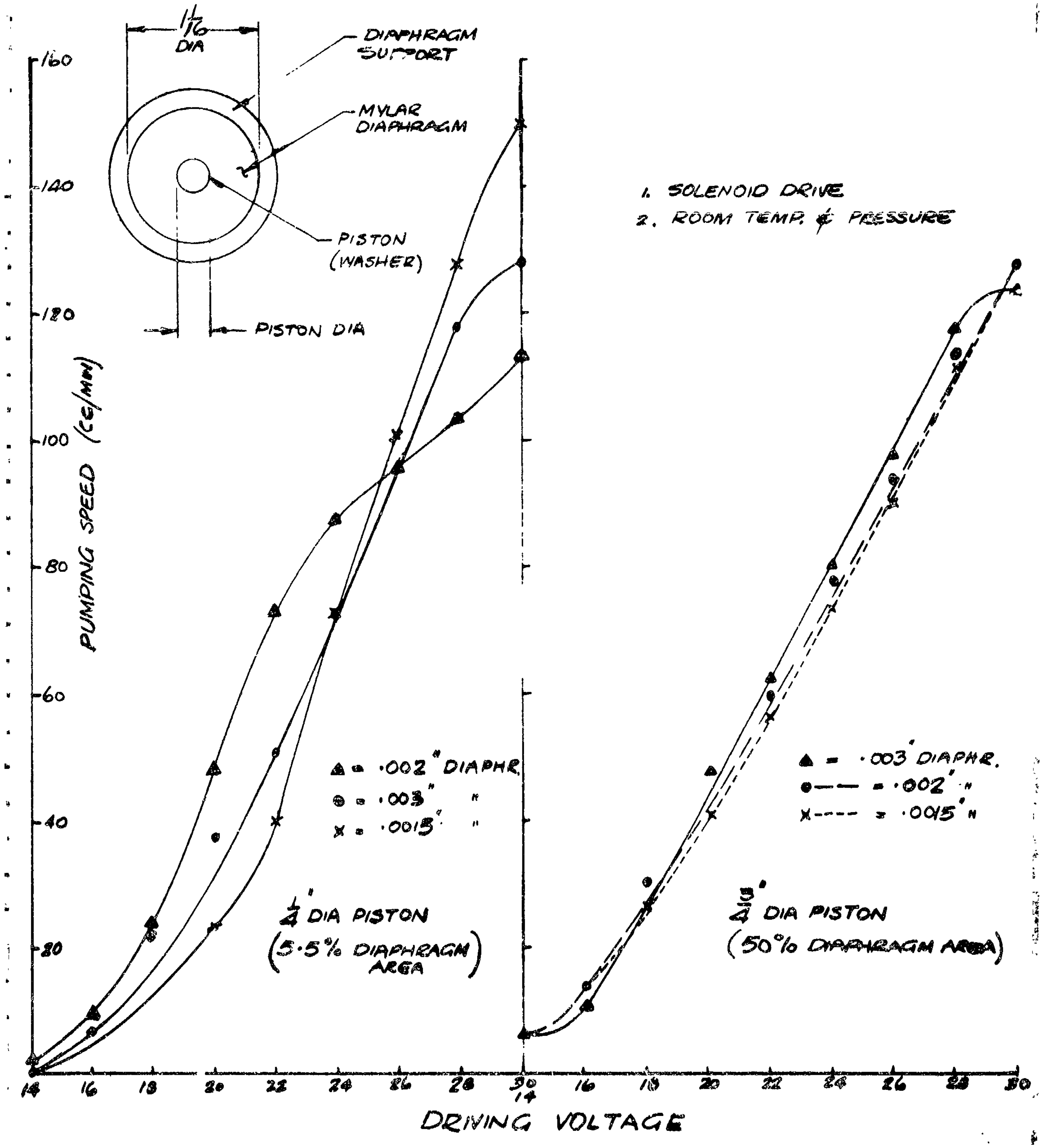

FIG 3.2 - PUMPING SPEED VS. DRIVING VOLTAGE FOR VARIOUS DIAPHRAGM THICKNESSES

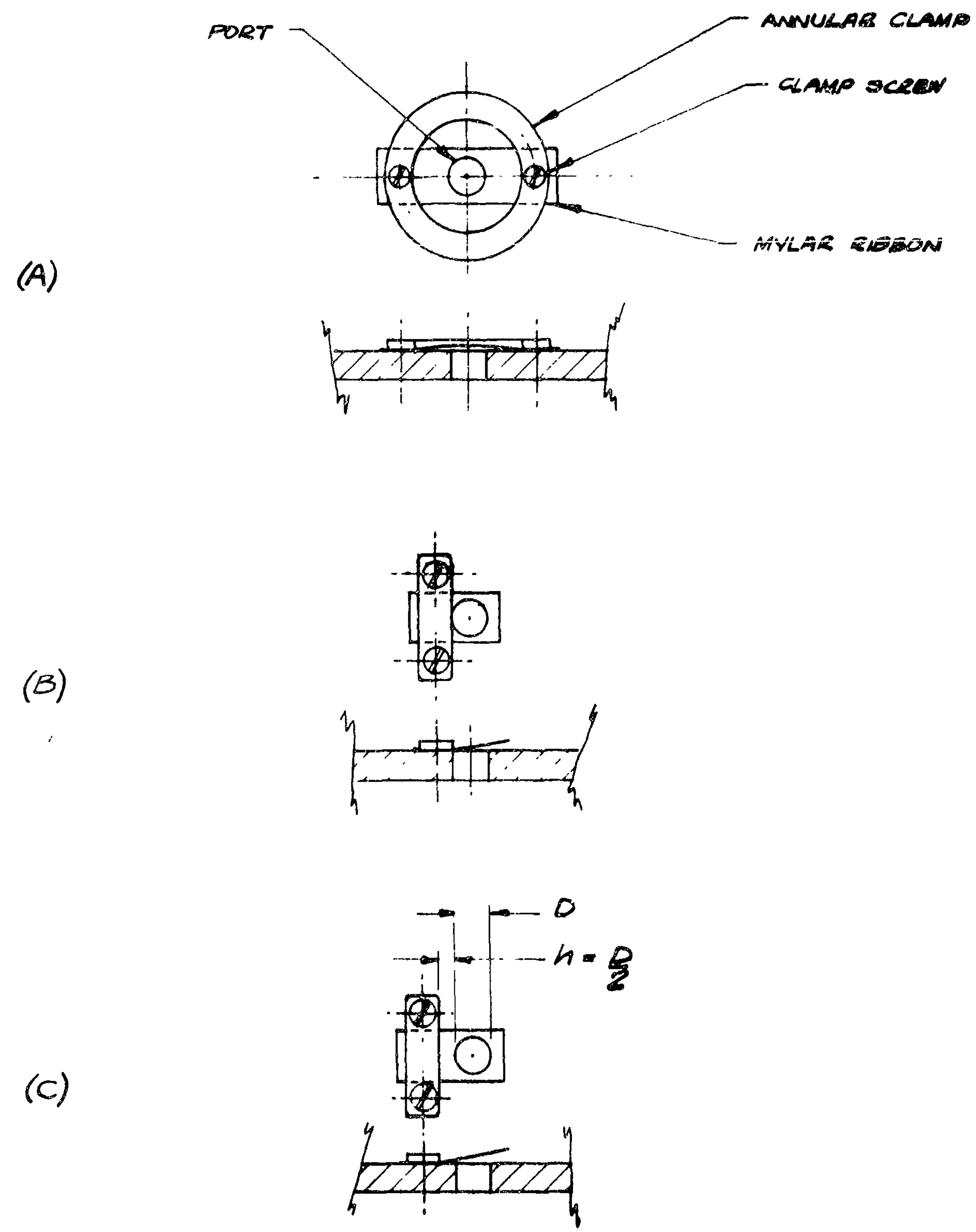

FIG 3.3 FLAPPER VALVE SUPPORTS

diaphragm size and configuration for the particular humidity probe load and driver (motor, solenoid, acoustic speaker, etc.) combination.

The diaphragm driver produces a force which is resisted by the spring constants of the system and the differential pressure appearing across the diaphragm during the intake and exhaust strokes. Sources of these forces are illustrated for an intake stroke in Fig. 3.4 using an acoustic speaker type drive unit.

The resulting motion of the diaphragm can be obtained from Newton's Force-Acceleration Equation, i.e.:

$$F_c - K_c S - K_D S - A_e (P_o - P_i) = M_e A_e \qquad (1)$$

where:

F_c	= Input force of voice coil.
S	= Displacement of coil and diaphragm from neutral position.
$-K_c S$	= Elastic restraining force due to voice coil supports.
$-K_D D$	= Elastic restraining force due to diaphragm material.
A_e	= Effective area of diaphragm which acts as a piston.
P_o	= Pressure outside of pump.
P_i	= Pressure inside of pump.
$-A_e(P_o - P_i)$	= Restraining force due to pressure differential across diaphragm.
M_e	= Moving mass consisting of voice coil, diaphragm, linkage, etc.
A_e	= Acceleration of M_e.

The pressure differential $(P_o - P_i)$ is dependent upon displacement (S) and dS/dt thus,

$$\Delta (P_o - P_i) = P = f\left(S, \frac{dS}{dt}\right) \qquad (2)$$

then

$$F_c - K_c S - K_D S - A_e f\left(S, \frac{dS}{dt}\right) = M_e A_e \qquad (3)$$

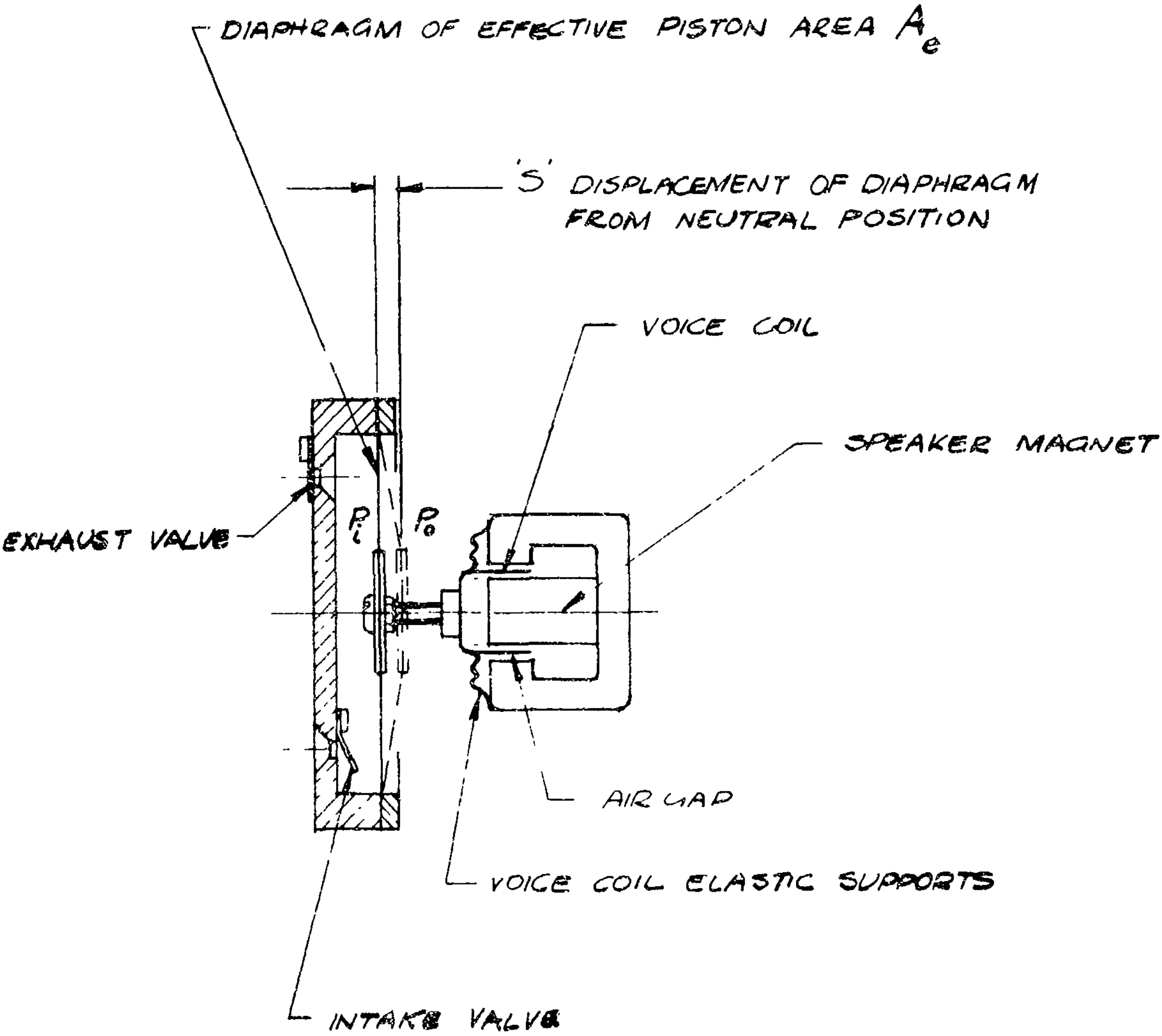

FIG 3.4 - SCHEMATIC DIAGRAM OF ACOUSTIC SPEAKER DRIVER & PUMP.

$\Delta P = f(S, dS/dt)$ is rather difficult to determine because of turbulence and drag forces introduced by the air moving through the humidity probe, connecting tubing, and intake flapper valve. A first order approximation which greatly simplifies the analysis is to assume $\Delta P = f(S)$. This simplication leads to the relationship

$$\text{Pumping Speed} \propto \frac{A_e}{1 + A_e^{\,2}} \tag{4}$$

assuming all other parameters such as driving force, driving frequency, etc. are constant. Normalizing the pumping speed at 350 cc/min for a diaphragm diameter of 1.25 in. yields the curve shown in Fig. 3.5. An experimental curve obtained by varying the diaphragm diameter at a fixed sinusoidal frequency and amplitude applied to the voice coil of a speaker drive is shown in Fig. 3.6. This curve corresponds very well with the theoretical curve thus verifying the existence of an optimum diaphragm size for particular load and driver combination.

Since the diaphragm is constructed of 1 mil Mylar, it is necessary to place a washer in the center of the diaphragm to form a rigid piston thus reducing the Mylar diaphragm to a narrow annular ring which acts as a flexible seal between the washer and the pump outer wall, as illustrated in Fig. 3.7. Three different sizes of washers were then tested to obtain maximum pumping speed as shown in the curves of Fig. 3.7.

The foregoing discussion, analysis and experimental data combine to specify the optimum diaphragm configuration for the particular load, driver mechanism, pump housing, and valve system used--namely, a diaphragm 7/8" o.d. and a piston area 50% of the diaphragm area. The results clearly indicate the process to follow to optimize the pumping speed of any drive, pump chamber and valve system. Additional experimental data relating pumping speed with drive frequency and exhaust manifold dimensions is presented in the section of this report devoted to the voice coil drive.

PUMP POWER UNITS

Four different pump power units were designed, fabricated and tested. Results of these investigations are given below.

DC Motor Drive:

An extensive survey of existing motors was conducted with essentially negative results. That is, several fractional horsepower mil-spec motors which meet the environmental requirements are available; however, they require too much power by a factor of three or more. These motors were also too large in weight and size although redesign could improve these conditions. Model airplane motors were investigated and found to be most

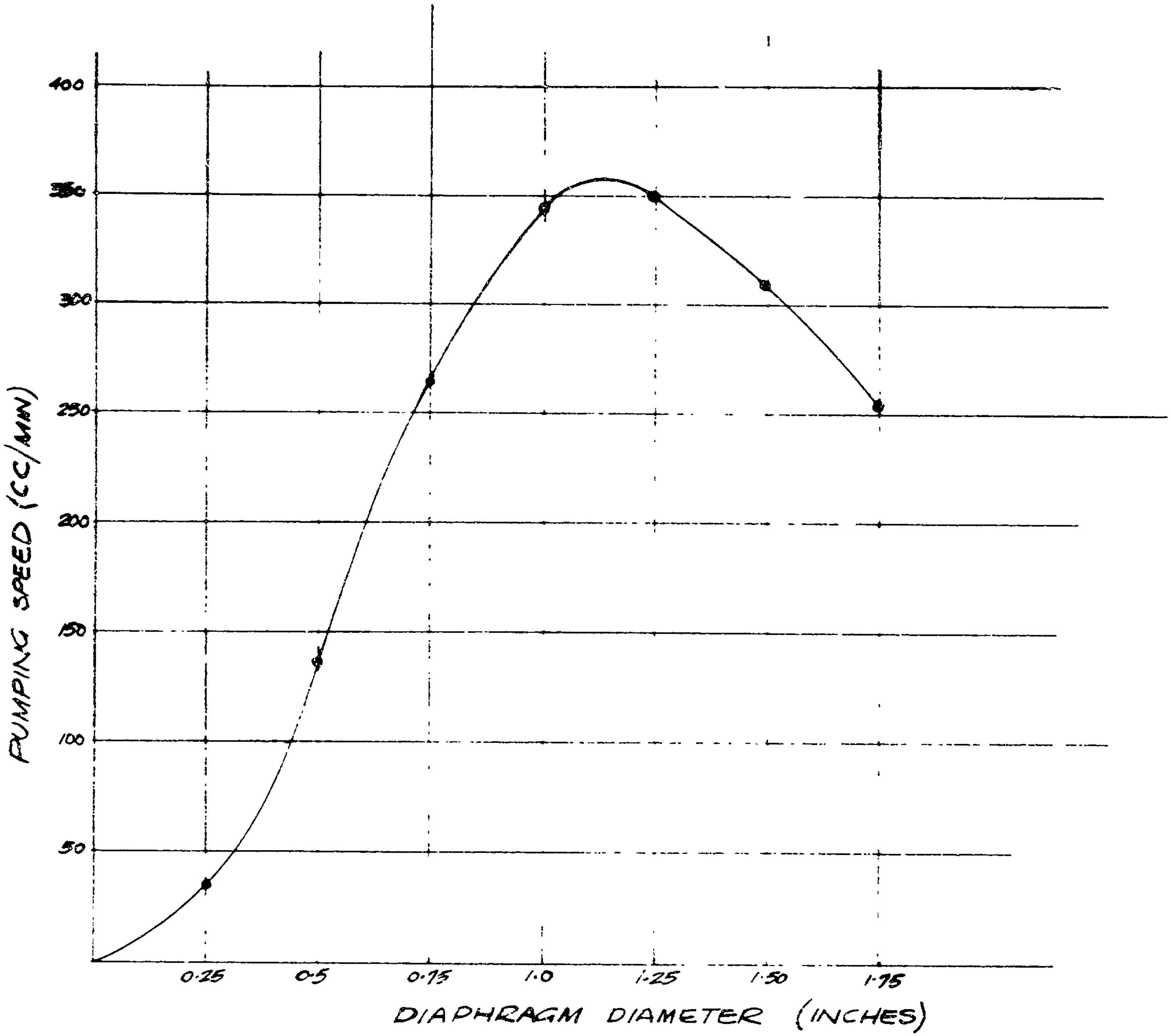

FIG 3.5 - PUMPING SPEED VS. DIAPHRAGM DIAMETER
(NORMALIZED @ 350 ML/MIN, 1.25" DIA)

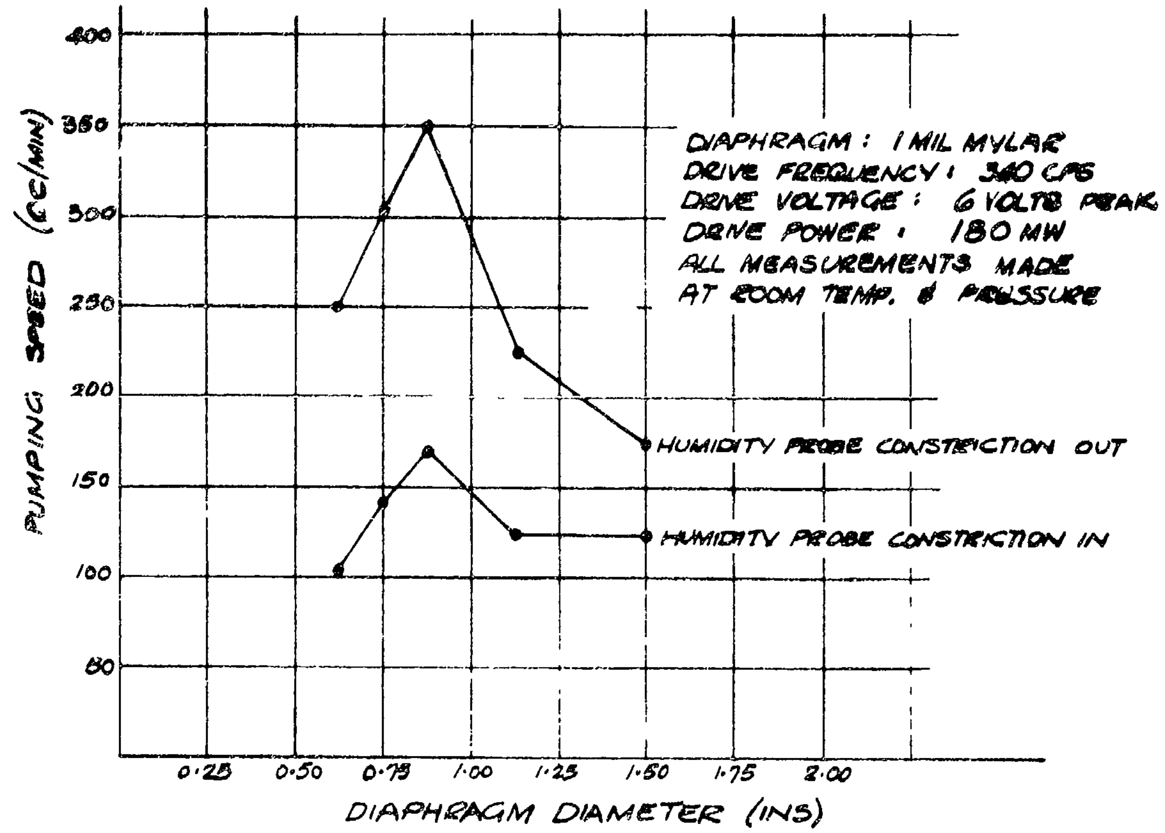

FIG 3.6 - PUMPING SPEED Vs. DIAPHRAGM DIA. (EXPERIMENTAL)

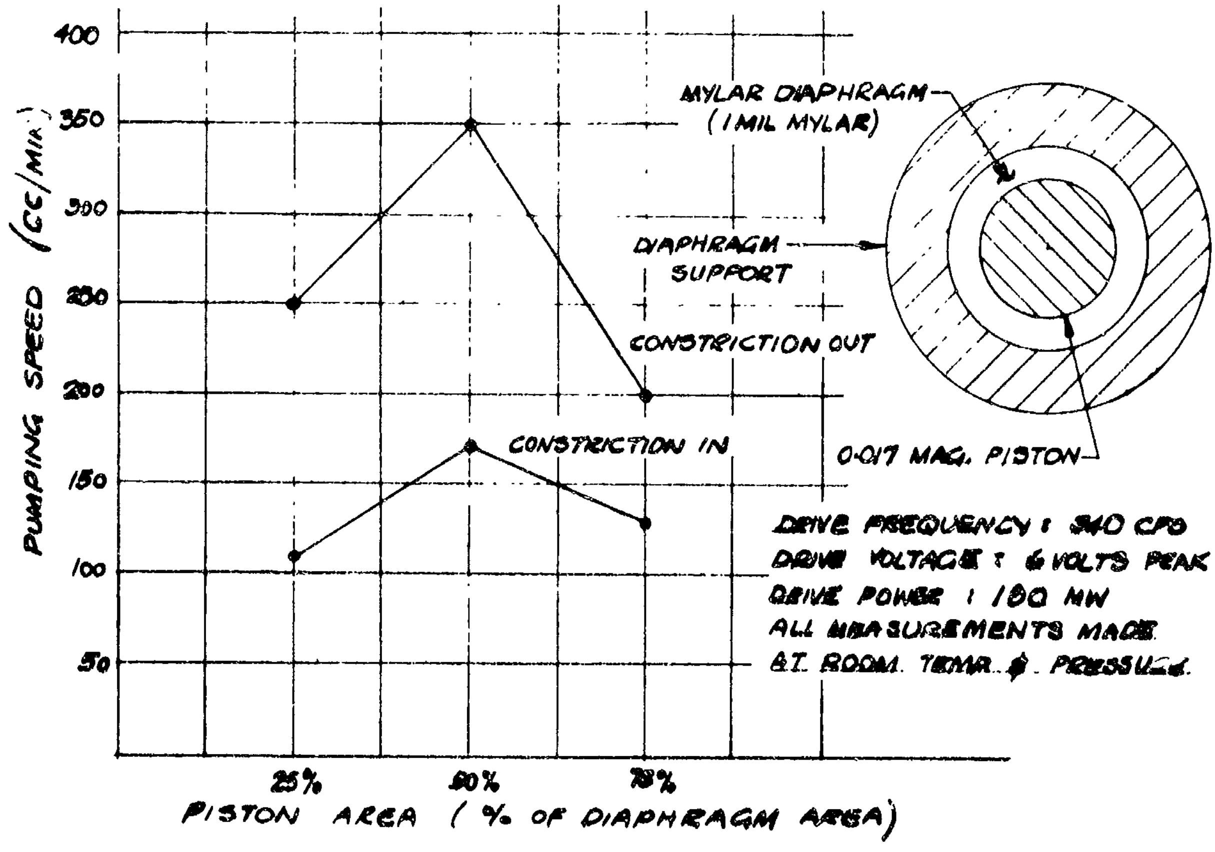

promising since they are small, light in weight, and operate on less than 250 mw of power. Three motors were tested by connecting them with a simple crank (Fig. 3.8) to a 1 mil Mylar diaphragm (1 1/16" o.d.) and valve system. Results are tabulated in Table 3-I.

The two Micro-Mo motors were fitted with gear boxes which reduced the output shaft speed to such a low value that the pump moved air through the system in pulses. However, previous experience with other un-geared Micro-Mo motors indicates that sufficient torque would be available to drive the diaphragm direct.

Results of the Distler motor drive tests conducted at low pressures appear in Table 3-II. These data indicate that reasonable pumping speeds, i.e., of the order of 1 to 2 cc/min, can be obtained at a pressure of 0.01 ATM. with a small diaphragm pump with a power expenditure of less than 250 mw. An effective piston diameter of 2 in. moving with a peak amplitude of approximately 0.1 in. at a frequency of approximately 100 cps should produce the desired flow at 0.01 ATM. Power distribution measurements indicate that approximately 143 mw of power is expended pumping air through the humidity probe, pump and connecting tubing at 0.03 ATM. at a rate of 0.8 cc/min while the motor, connecting linkage, and piston washer absorbed an additional 59 mw. Careful design of the piston and drive mechanism could reduce this loss to 40 mw or less; thus providing at least 210 mw for movement of the air assuming the maximum power available is 250 mw.

These tests clearly indicate that a DC electric motor can be used provided the permanent field magnets can be shielded and the motor components can be modified to meet the environmental conditions. At the present time, it appears that both these problems can be satisfactorily solved.

AC Solenoid-Permanent Magnet Drive:

The alternating magnetic field produced by AC power applied to a coil was used to alternately pull and push a permanent ceramic magnet attached to the pump diaphragm as shown in Fig. 3.9. Various coils and magnets were used; however, significant results were obtained only with the coil and magnet indicated. A maximum pumping speed of 60 cc/min (room temperature and pressure) was obtained with an expenditure of 1 watt in the solenoid fitted with a soft iron core. Removal of the iron core reduced the pumping speed by approximately 50%.

Test results clearly indicate that the loose magnetic coupling between the solenoid and the magnet plus the wasted magnetic field at the opposite end of the solenoid is basically an inefficient arrangement, and although it can be improved upon, will not provide the proper pumping speeds at the required power level. In addition, the magnetic field of the ceramic magnet

(A)

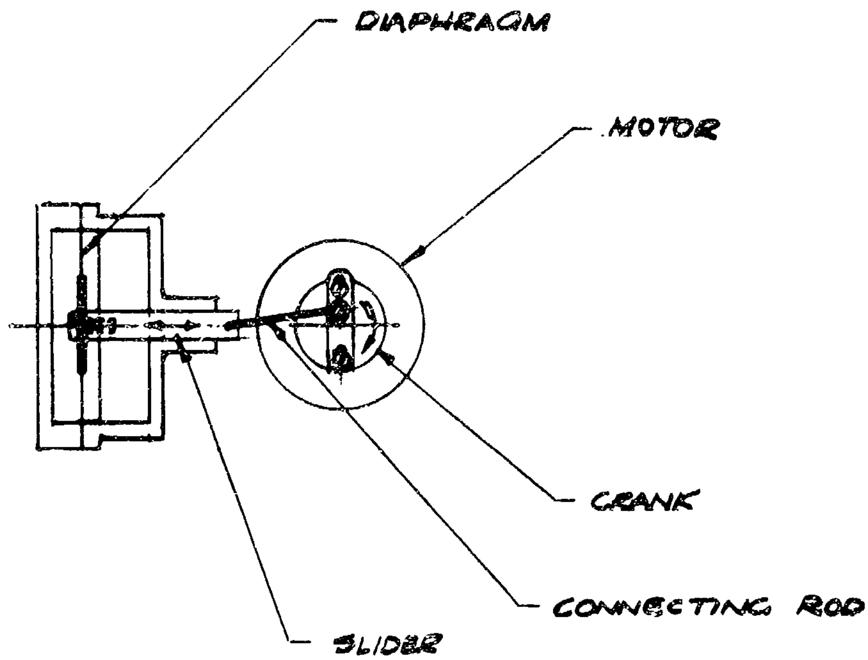

(B)

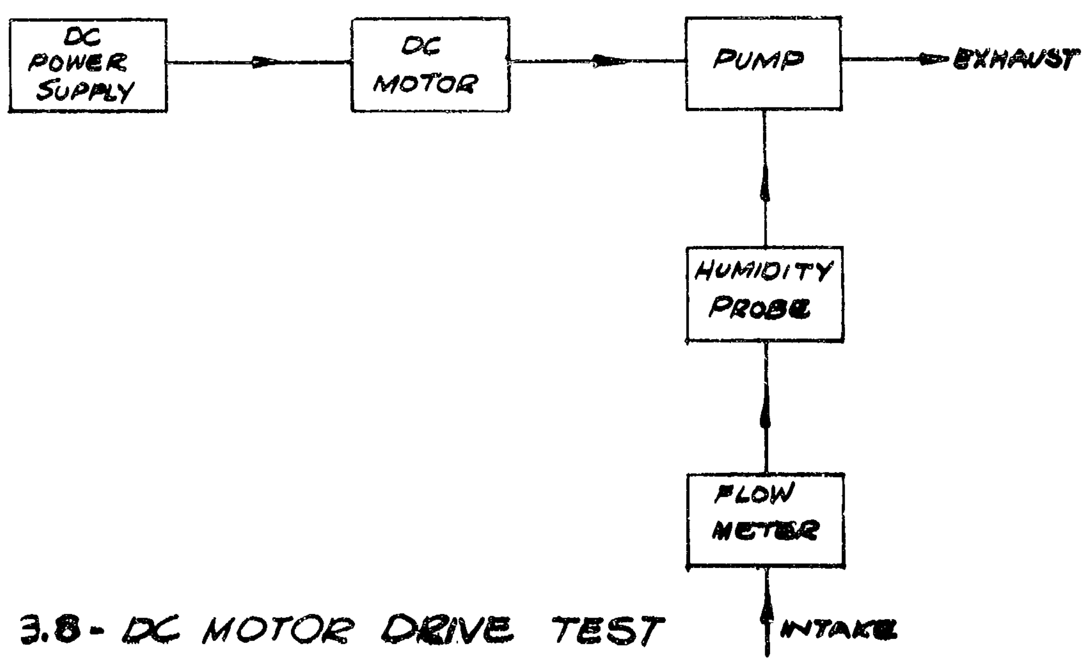

FIG 3.8 - DC MOTOR DRIVE TEST CONFIGURATION

(A)

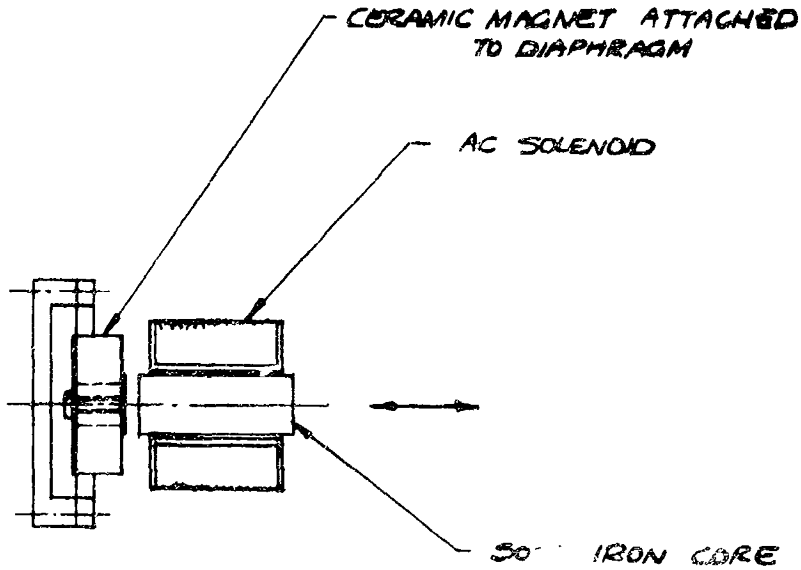

NOTE: THE DIAPHRAGM PUMP, HUMIDITY PROBE & FLOWMETER ARE THE SAME AS USED IN THE DC MOTOR TESTS.

(B)

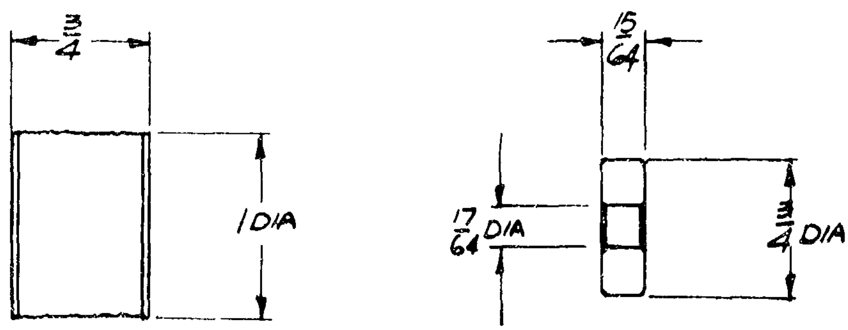

SOLENOID COIL SPECIFICATIONS
VOLTAGE: 6 VAC 50-60 CPS
WEIGHT: 2 OZ

MAGNET SPECIFICATIONS
MAT'L INDOX I
WEIGHT: 1/4 OZ

FIG 3.9 - AC SOLENOID - PERMANENT MAGNET DRIVE

TABLE 3-I

DC MOTOR DRIVE PERFORMANCE TEST RESULTS

Type	Dimen. (Inches)	Wt. (Oz.)	Volts (DC)	Output Shaft Speed (RPM)	Power (MW)	Dphrgm. Ampltd. (Inches)	Flow (ML/Min)	Comments
Micro-Mo	9/16 x 1	0.5	1.5	64	70	0.023	Pulse	Pumping rate too slow to obtain steady reading.
"	"	"	3.0	120	510	0.023	Pulse (Av. 60)	
Micro-Mo	3/4 x 1	1.0	1.5	169	40	0.023	Pulse (Av. 50)	Pumping rate too slow to obtain steady reading.
"	"	"	3.0	341	178	0.023	Pulse (Av. 60)	"
Distler	1 x 2 1/2	2.75	1.5	1410	64	0.023	160	Smooth flow observed.
"	"	"	3.0	3160	150	0.023	200+	"

Note: All measurements were made at room temperature and pressure.

TABLE 3-II

DISTLER MOTOR DRIVE TESTS AT LOW PRESSURES

PRESSURE (ATM)	VOLTAGE (VDC)	CURRENT (MA)	POWER (MW)	RPM	PUMPING SPEED CC/MIN Corrected to STP
0.01	4.5	45	202	4700	0.0
0.03	4.5	45	202	5700	0.8
0.07	4.5	45	202	5200	12.0
0.12	3.0	80	240	2700	23.0
0.20	2.5	80	200	2300	36.0

Diameter of Diaphragm = 1 1/2"
Diameter of Washer Piston = 1 1/16"
Amplitude of Washer Piston = $\sim$ 0.045"
Temperature = 80°F

POWER DISTRIBUTION AT 0.03 ATM. PRESSURE

CONFIGURATION	RPM	POWER (MW)
Complete System	5700	202
Humidity Probe Constriction Removed	5700	76
Mylar Diaphragm Removed	5700	59
Motor Only	5700	31

and the induced field of the iron core would require substantial shielding to reduce it to the required level of one gamma at a distance of four feet.

Both ceramic and Alnico magnets will retain their magnetic properties when subjected to the various environmental conditions and therefore can be used in other more efficient devices. Some of the important properties of these two materials are listed in Table 3-III.

Linear Motion DC Solenoid:

Conventional linear motion DC solenoids were investigated in detail because they can be constructed to use little power, make efficient use of the magnetic field produced by the coil, exhibit very small residual magnetic fields in the off condition, are small, light weight, and production units presently on the shelf meet or exceed all environmental requirements. Of the many solenoid manufacturers contacted, two* had existing models which meet the requirements. IMC Magnetics had two units in stock which were purchased for testing purposes. Details of this model are given below and in Fig. 3.10.

SPECIFICATIONS OF IMC SOLENOID 4SD819-3

Voltage Range:	18 to 30 VDC
Current:	Actuating 0.030 amps at 24 VDC at 78°F
Rated Force:	Pull 10 grams at 0.030 stroke at 24 VDC at 78°F
Duty Cycle:	Continuous
Temperature Range:	-65°F to 165°F Note: Can bake at 300°F and will operate at 212°F for approximately one-half hour. Higher temperature units can be produced with special materials.
Weight:	Unit 10 grams, Plunger 1 gram

This solenoid was attached to the diaphragm as shown in Fig. 3.11 and driven by a transistorized square wave oscillator shown in Fig. 3.12. Preliminary environmental temperature and voltage checks of the oscillator appear in Table 3-IV.

* Cannon Electric and IMC Magnetics Corporation.

TABLE 3-III

MAGNETIC AND PHYSICAL PROPERTIES OF ALNICO V AND INDOX I

	ALNICO V	INDOX I
Peak Energy Product $B_d H_d$ (MAX) x 10^6	5.25	0.8
Residual Induction B_r, (Kilogauss)	12.5	2.0
Coercive Force H_c, (Oersteds)	600	1,600
Ability to withstand demagnetizing fields	Good	Exceptional
Approximate Temperature permanently affecting material, (°F)	1,000	1,800
Density (cb/cu. in.)	0.265	0.167
Mechanical Properties	Hard--Brittle	Hard--Brittle
Electrical Resistivity (Microhm-cm at 25°C)	47	10^{12}
Tensile Strength (lb/sq. in.)	5,450	Low
Shape Limitations	Cast	Pressed
Machinability	Grind Only	Grind Only

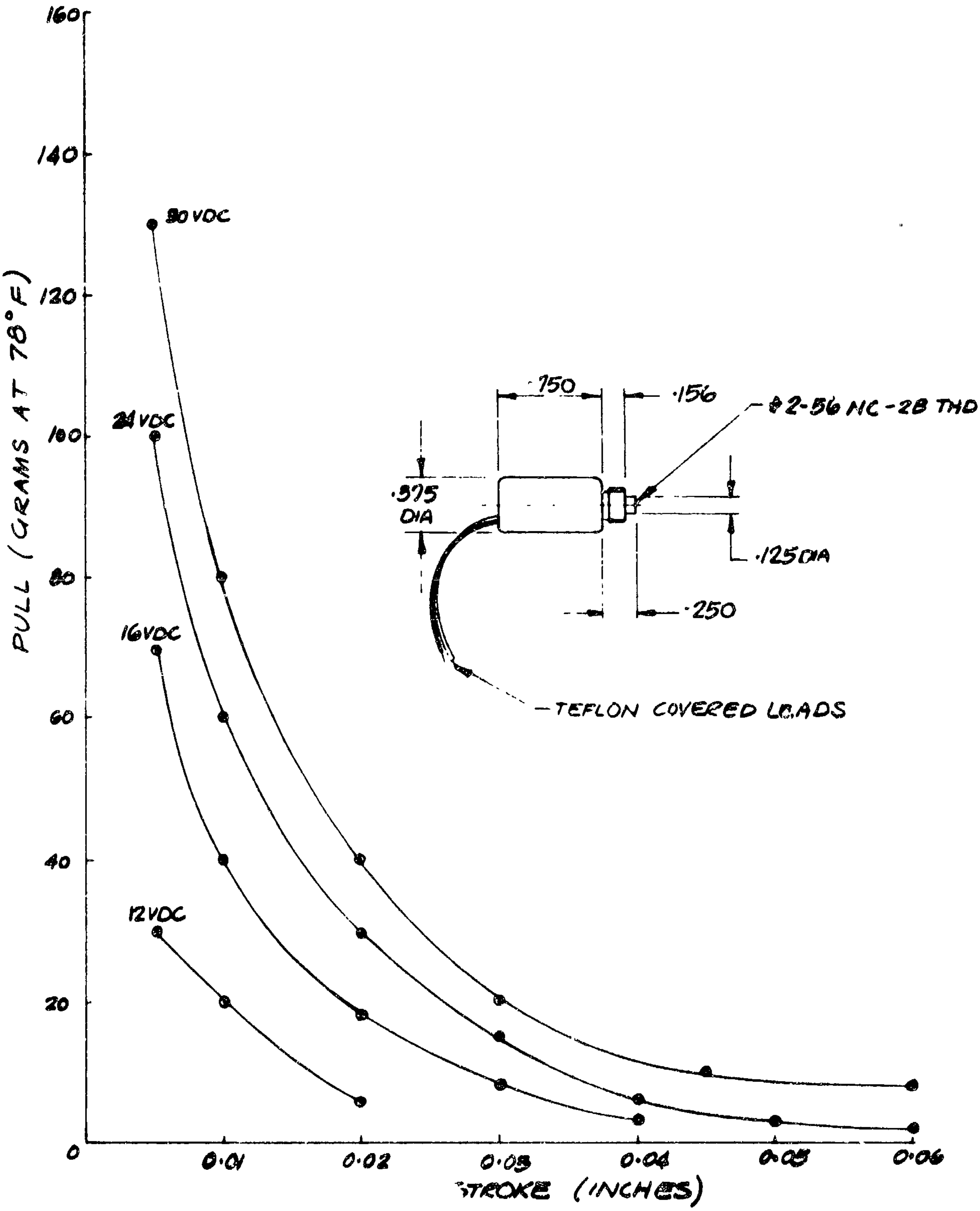

FIG 3.10 - STROKE VS. PULL, LINEAR DC SOLENOID 4SD 819-3

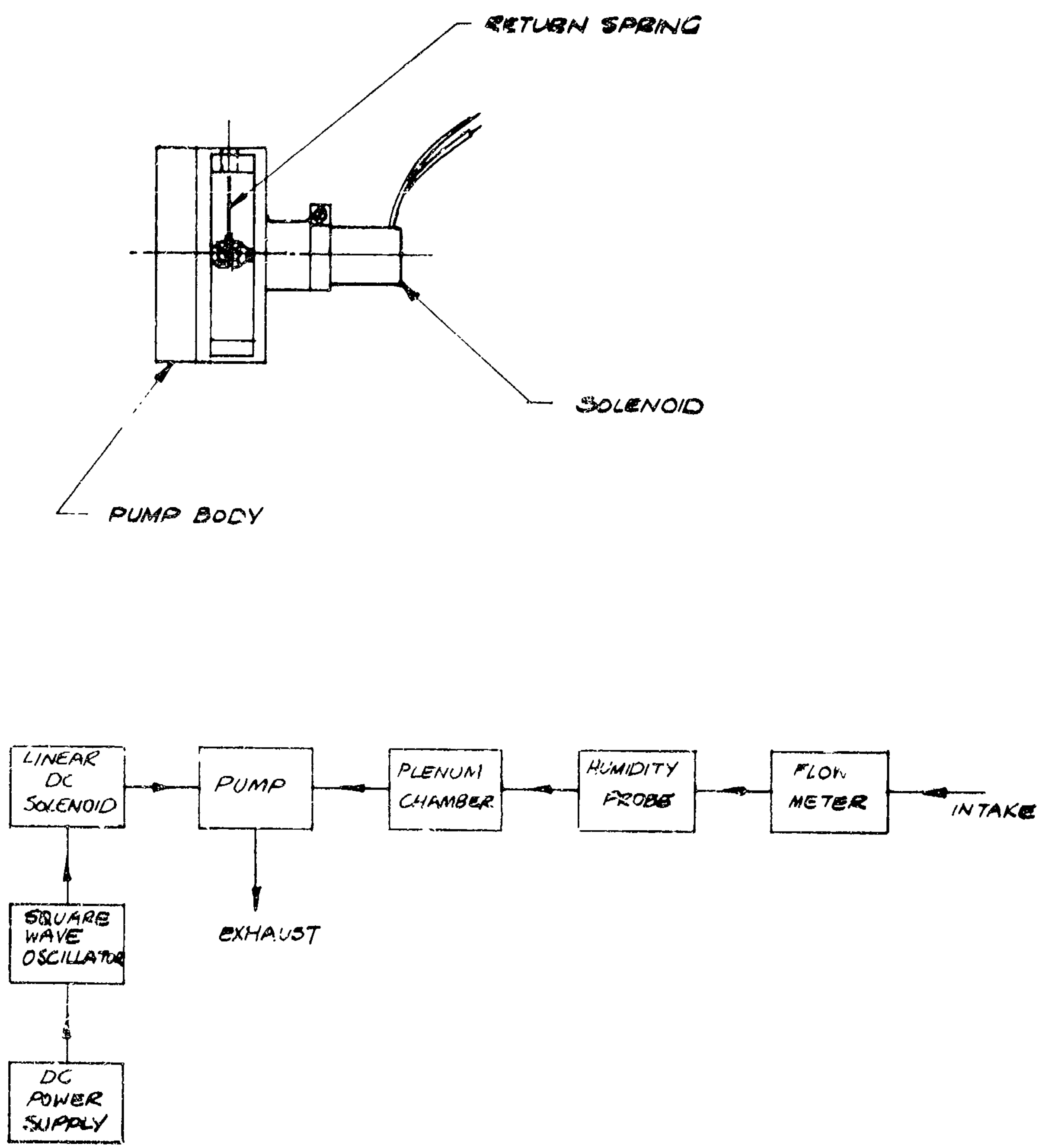

FIG 3.11 - LINEAR DC SOLENOID PUMP DRIVE SYSTEM

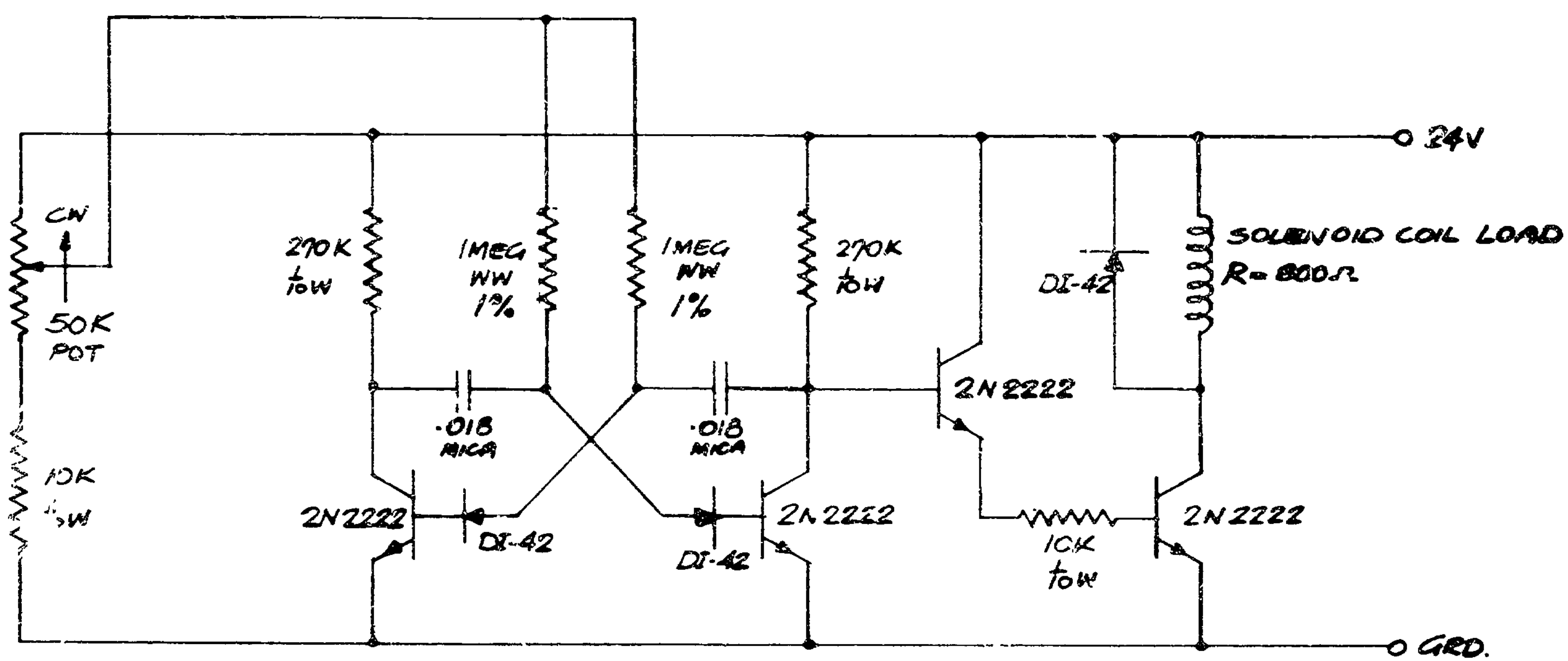

FIG 3.12 - VARIABLE FREQUENCY SQUARE WAVE OSCILLATOR

TABLE 3-IV

PRELIMINARY OSCILLATOR ENVIRONMENTAL CHECKS

AMBIENT TEMPERATURE	FREQUENCY	INPUT VOLTAGE	FREQUENCY
-20°C	29.9 cps	15 VDC	29.6 cps
+30°C	30.0 cps	24 VDC	30.0 cps
+100°C	30.2 cps	30 VDC	30.1 cps
+150°C	30.6 cps	30 VDC	30.1 cps

Results of pump performance tests are shown in Fig. 3.13. Analysis of these performance curves combined with operational knowledge gained during the mechanics of collecting the data leads to the following conclusions and comments:

1. A linear DC solenoid can actuate the diaphragm pump at a power level of less than 250 mw while maintaining a steady flow of at least 100 cc/min at room temperature and pressure.

   In particular, the IMC Magnetics model 4SD819-3 solenoid has maintained a steady flow of 100 cc/min at room temperature and pressure at 18 VDC with a duty cycle of 50% and an average power consumption of 202 mw. This is increased performance over that indicated in Fig. 3.13 and was accomplished by addition of a plenum chamber between the pump input and the humidity probe (see Fig. 3.11). The volume of air in the plenum chamber acts as a filter to smooth differential pressure pulses which appear on the diaphragm during the intake stroke. If the pump looks directly into the humidity probe constriction then the diaphragm will be subjected to differential pressure pulses sufficient to restrict its motion and thereby change the pumping speed. In one particular test, the pumping speed was increased from 60 cc/min to 100 cc/min by the addition of a 5 cc plenum chamber. This effect is peculiar to the solenoid drive because of the critical dependence of the plunger force on the displacement of the plunger from the bottom position. Without a plenum chamber the differential pressure on the diaphragm causes the plunger to assume a new average position further away from the bottom position in the solenoid. The force on the plunger is thereby reduced, which results in less plunger motion and consequently less pumping speed.

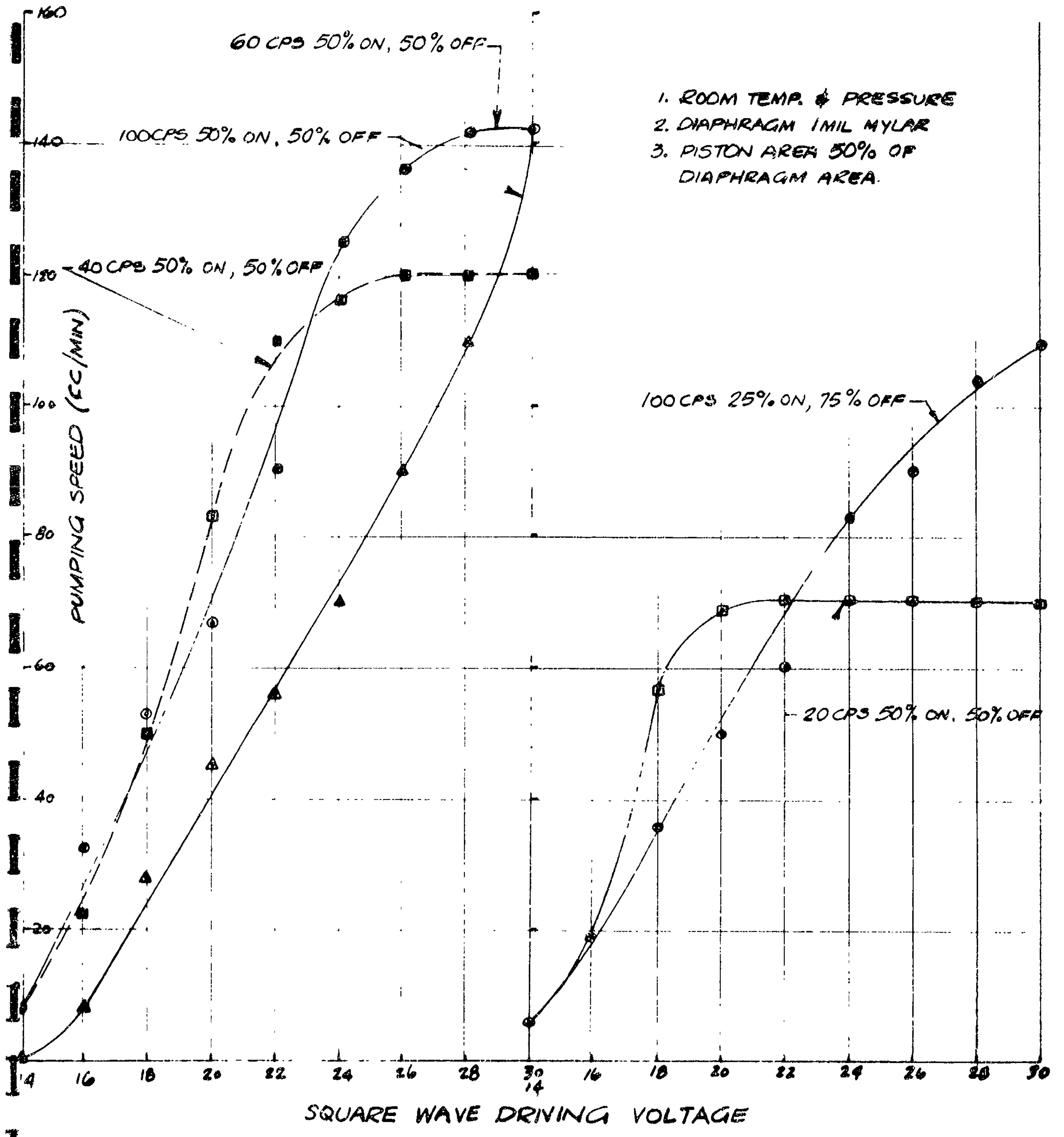

FIG 3.13 - PUMPING SPEED vs. DRIVING VOLTAGE AT VARIOUS FREQUENCIES & TWO DUTY CYCLES (LINEAR DC SOLENOID DRIVE)

2. As stated above, the magnetic coupling between the plunger and coil armature is critically dependent upon plunger position, requiring stiff supports between the diaphragm structure and the solenoid case. The solenoid must be positioned while running to obtain optimum performance, and a clamping arrangement designed which does not shift the solenoid case during the clamping operation.

3. Friction forces between the plunger and solenoid case have a pronounced effect upon pumping speed, requiring accurate alignment of plunger and case as well as polishing both surfaces. Dry lubricants or coating the surfaces with teflon would further increase pumping efficiency.

4. Further development work on a solenoid specifically designed for this purpose would produce improvements in pumping speed with less consumption of power. Several possible approaches are listed below:

   a. Investigate various solenoid coil shapes to obtain maximum magnetic field energy with the power available.

   b. Contour the plunger and solenoid armature to obtain a more linear stroke vs pull curve.

   c. Vent the volume contained by the armature and plunger to prevent enclosed air from compressing and thus retarding the motion of the plunger.

   d. Investigate the efficiency of dividing the input power between two opposed solenoids in order to drive the plunger during both the input and exhaust stroke and thus eliminate the return spring.

Acoustic Drive:

Utilizing the well-known electro-mechanical energy conversion phenomenon employed in acoustic speakers produced a pump drive unit that has wide performance limits, reasonable efficiency and can be made to survive more severe environmental conditions than those specified in this study. Basic components of this drive unit are shown in Fig. 3.4. Fortunately, a miniature commercial transistor radio speaker in the power range of 250 mw (Quam 22A06Z100) was available and a modified version was used for these performance tests.

Because this approach showed promise over other techniques given preliminary performance checks, more extensive tests were conducted.

Complete curves were obtained for the original unmodified speaker, and for a modified version in which three equal sections of the voice coil support were removed (Fig. 3.14). In all tests the speaker diaphragm was completely removed. The resulting performance curves are shown in Figures 3.15 through 3.23. Analysis of these curves combined with additional background information are summarized as follows:

Pumping Speed Control:

Pumping speed can be controlled in a continuous smooth manner by varying the amplitude or the duty cycle of the oscillatory drive at a fixed frequency. Both methods have been used in a servo loop to produce a steady mass flow as the ambient pressure is lowered toward 0.1 ATM. Amplitude modulation gave greater control range and is used in the feasibility breadboard model. Transistor drive systems are designed to produce square waves since transistors are more efficient when operated in the on-off switch mode than when operated in the proportional mode.

Pumping speed cannot be controlled in a proportional manner by varying the drive frequency due to combination of resonance effects, e.g., acoustic resonance of pump chamber and exhaust manifold, mechanical resonance of voice coil, voice coil supports, and diaphragm-piston system, resonance of flapper valves, and mechanical resonance of supports between the driver magnet and the pump housing.

Pumping Speed at Low Pressures:

Pumping speed at low pressures, shown in Fig. 3.23, can be improved by an order of magnitude by increasing the effective piston area and its amplitude. The optimization of the diaphragm size discussed earlier in this report was carried out at room temperature and pressure. Since the density is a function of pressure and temperature and the viscosity is a function of temperature, the optimization of the pump size and the area ratio of the washer piston will have to be accomplished in the expected reduced pressure and temperature environment. The pressure differential appearing across the diaphragm is correspondingly reduced as the pressure and viscosity are lowered, allowing the excursion of the diaphragm to increase. The excursion of the diaphragm in the present breadboard model is limited by the voice coil support which is constant and independent of pressure, thus limiting the pumping speed capabilities at low pressures, i.e., below 0.5 ATM. A detailed discussion of this type pump drive with the chief engineer of acoustic transducers of Altec Lansing Corporation revealed that the Quam driver we are using operates at an efficiency level of approximately 1% and that an acoustic voice coil specifically designed for this application would operate at an efficiency of from 20% to 25%. Use of special magnets and magnetic circuit materials would provide this increase

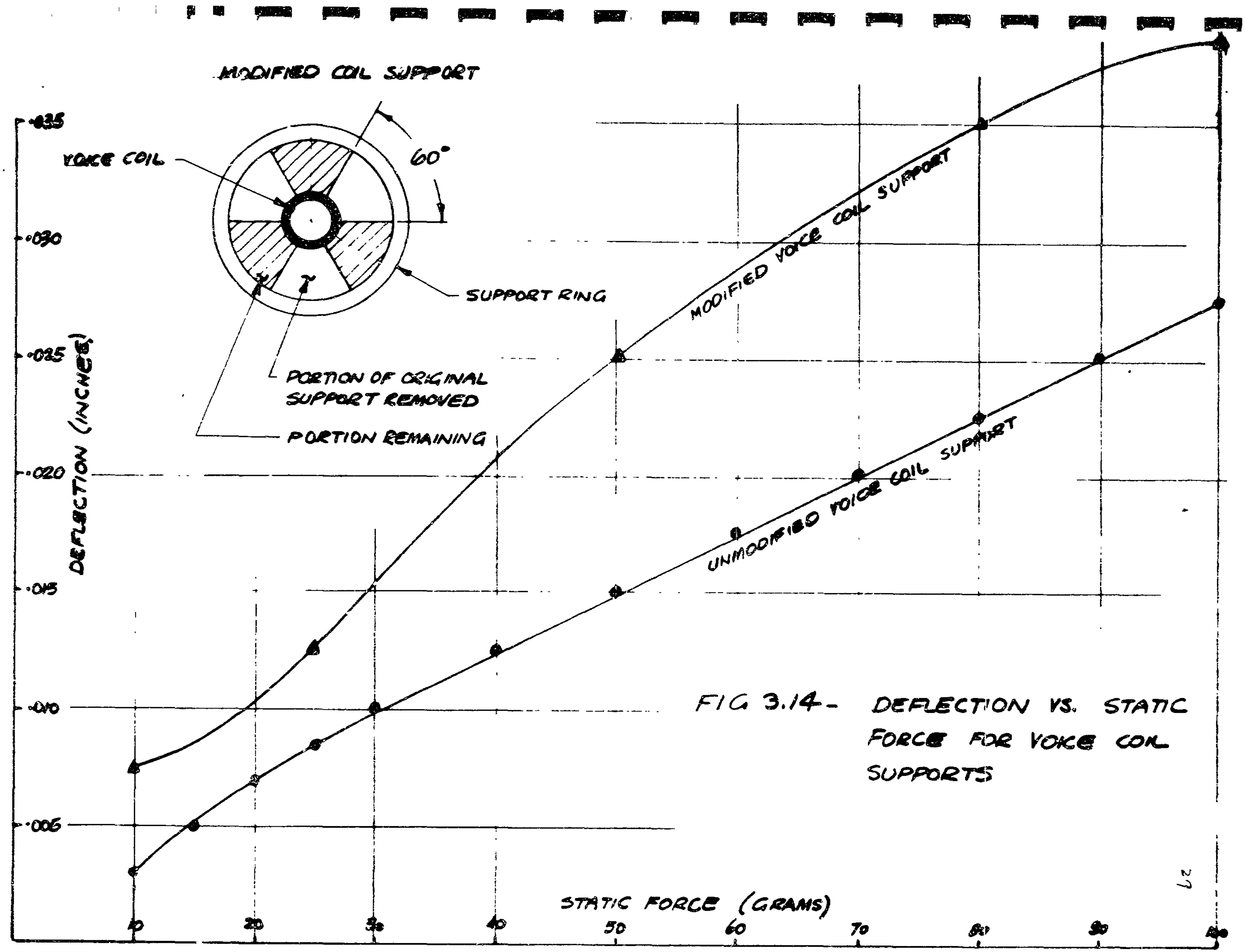

FIG 3.14- DEFLECTION VS. STATIC FORCE FOR VOICE COIL SUPPORTS

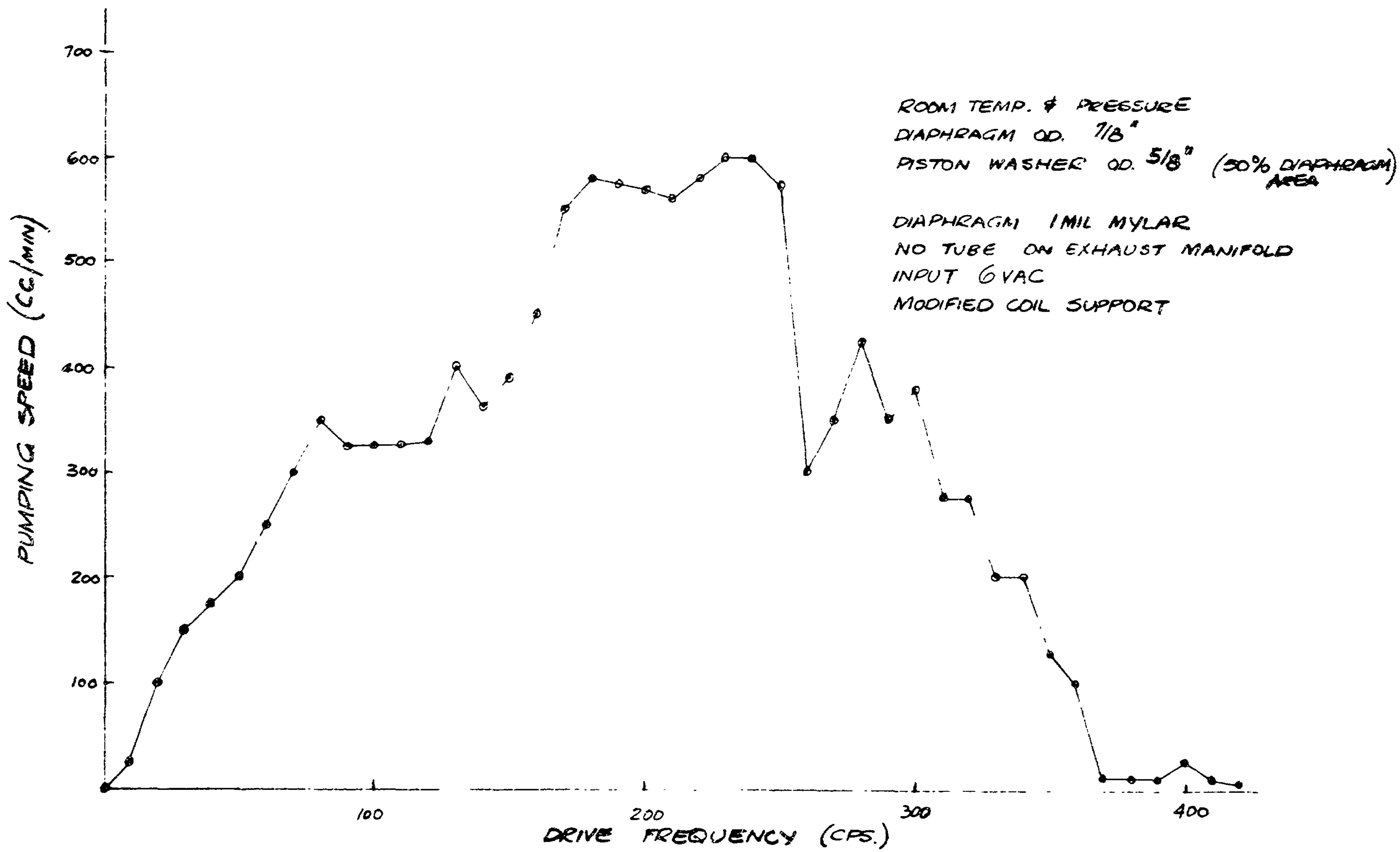

FIG 3.15 - PUMPING SPEED VS. DRIVE FREQUENCY
(HUMIDITY PROBE CONSTRICTION OUT OF SYSTEM)

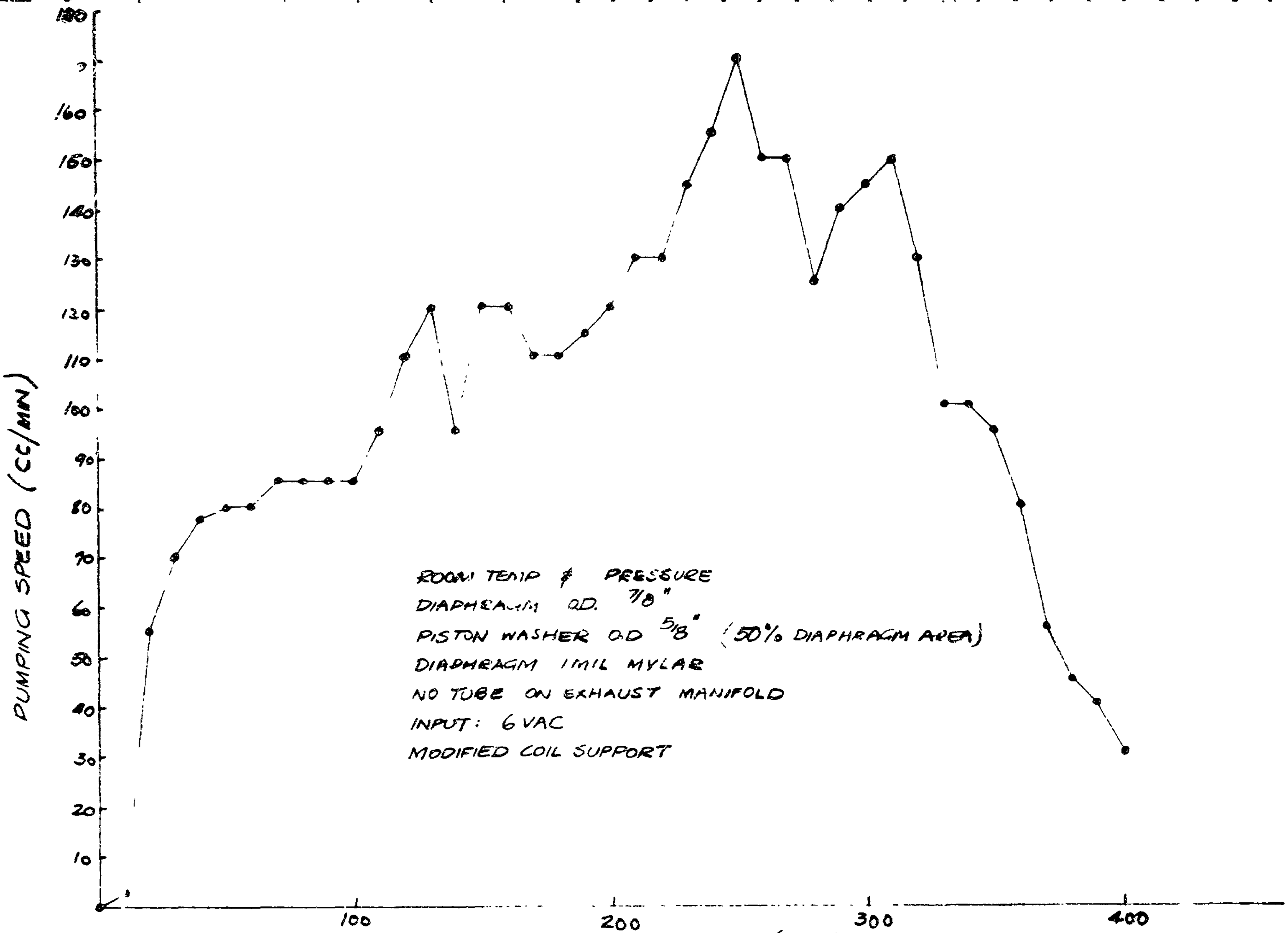

FIG 3.16 - PUMPING SPEED VS. DRIVE FREQUENCY
(HUMIDITY PROBE CONSTRICTION IN SYSTEM)

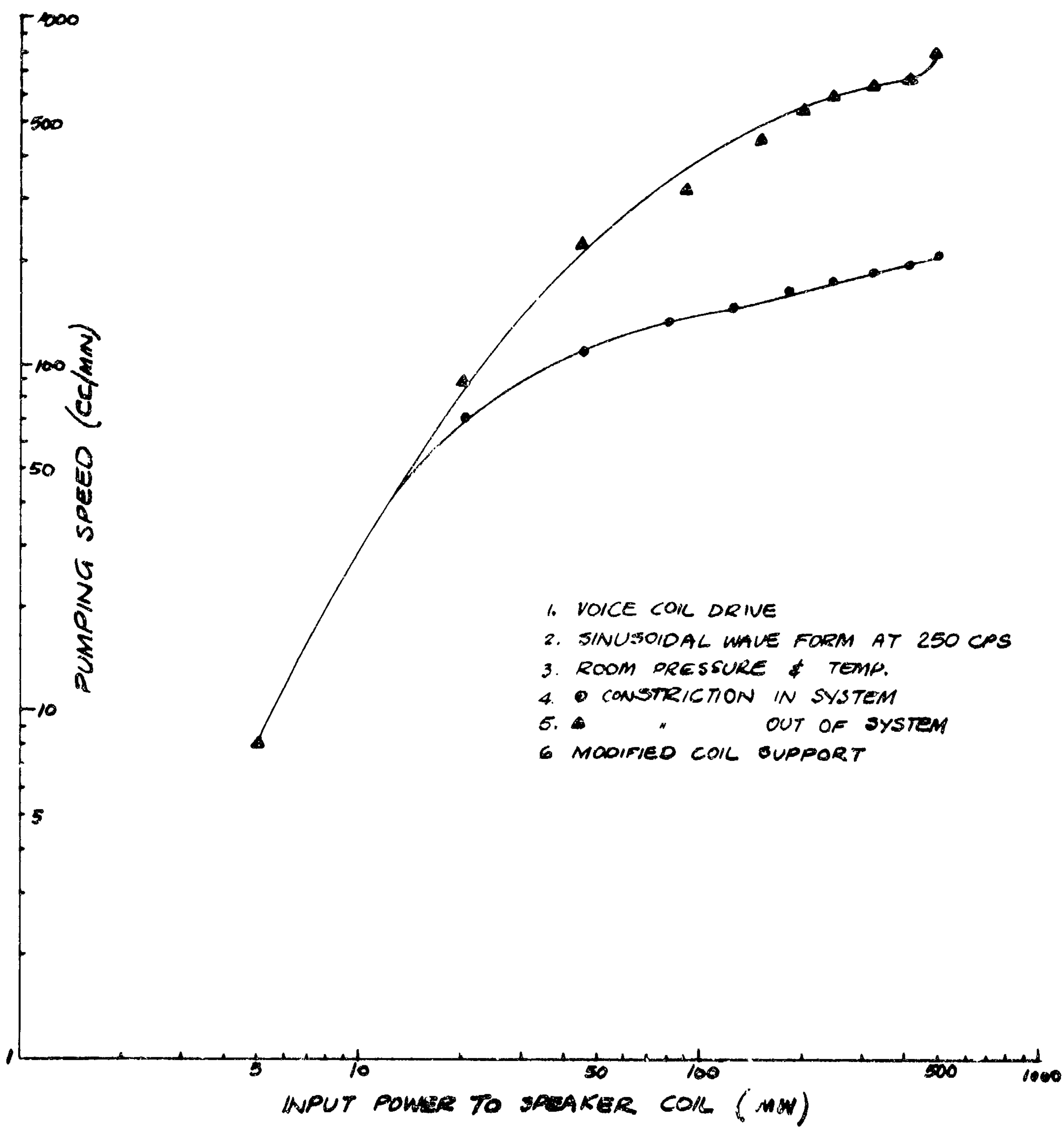

FIG 3.17 - PUMPING SPEED VS. INPUT POWER

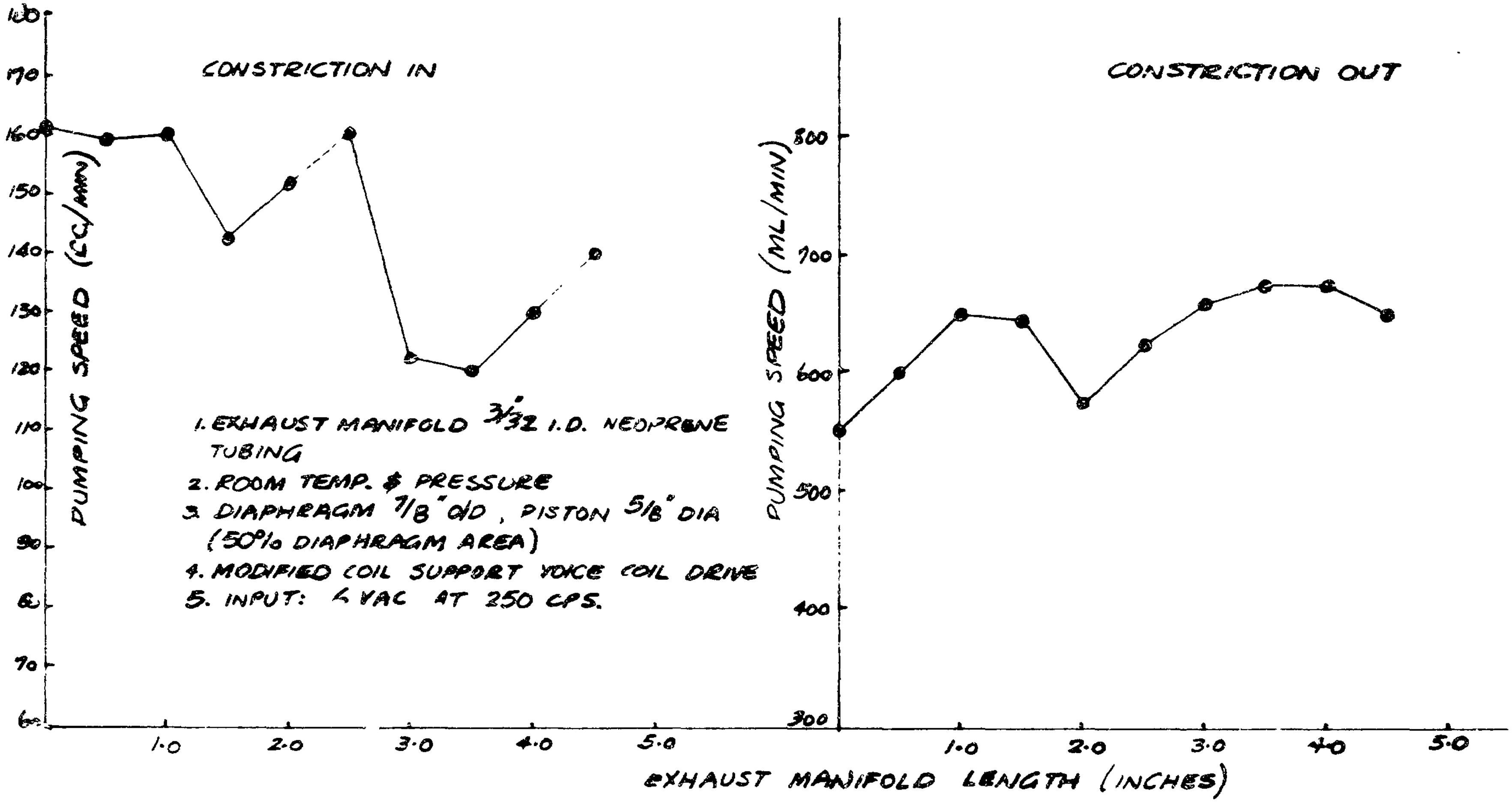

FIG 3.18 - PUMPING SPEED VS. EXHAUST MANIFOLD LENGTH.

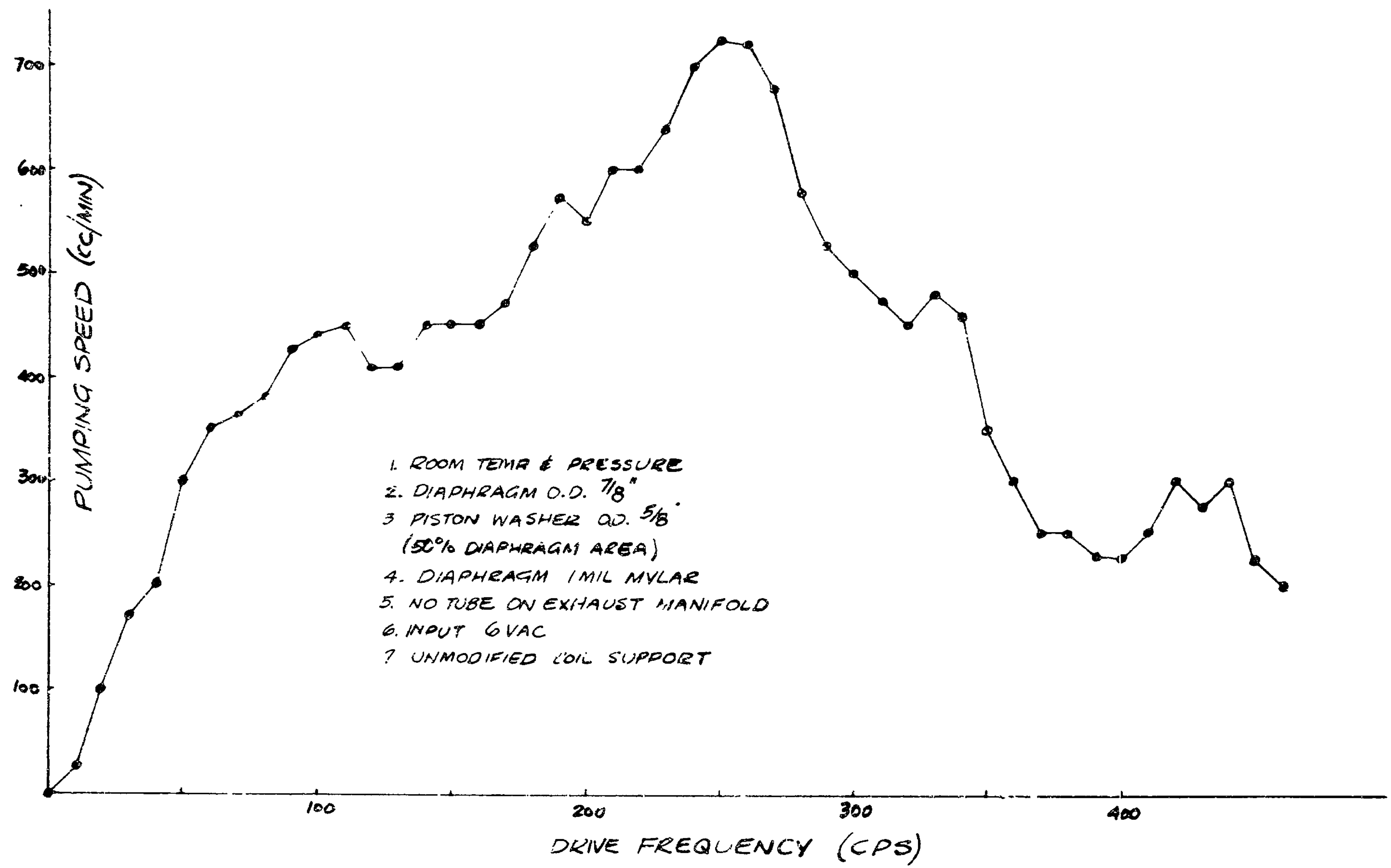

FIG 3.19 - PUMPING SPEED VS. DRIVE FREQUENCY
(HUMIDITY PROBE CONSTRICTION OUT OF SYSTEM)

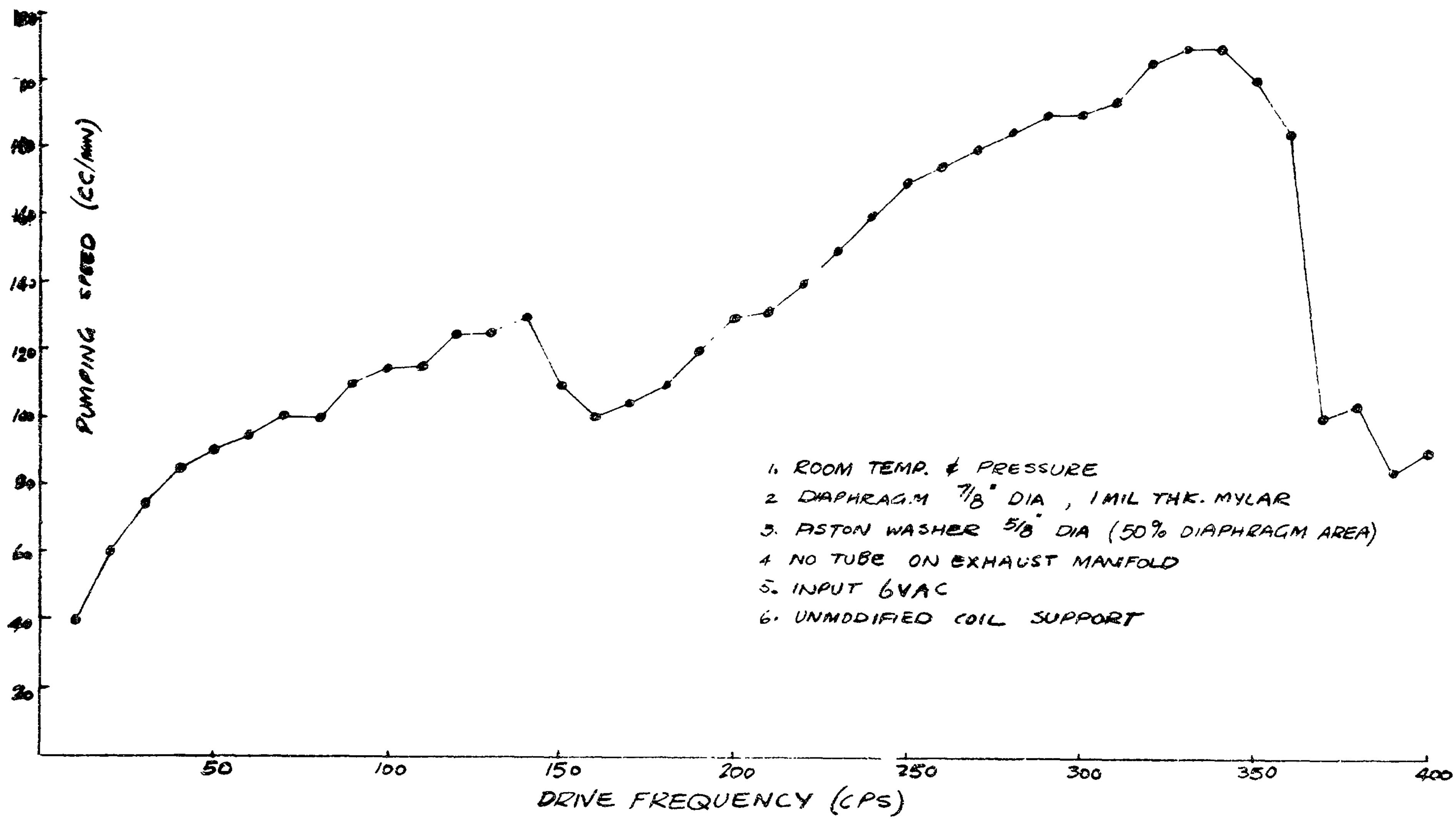

FIG 3.20- PUMPING SPEED VS. DRIVE FREQUENCY
(HUMIDITY PROBE CONSTRICTION IN SYSTEM)

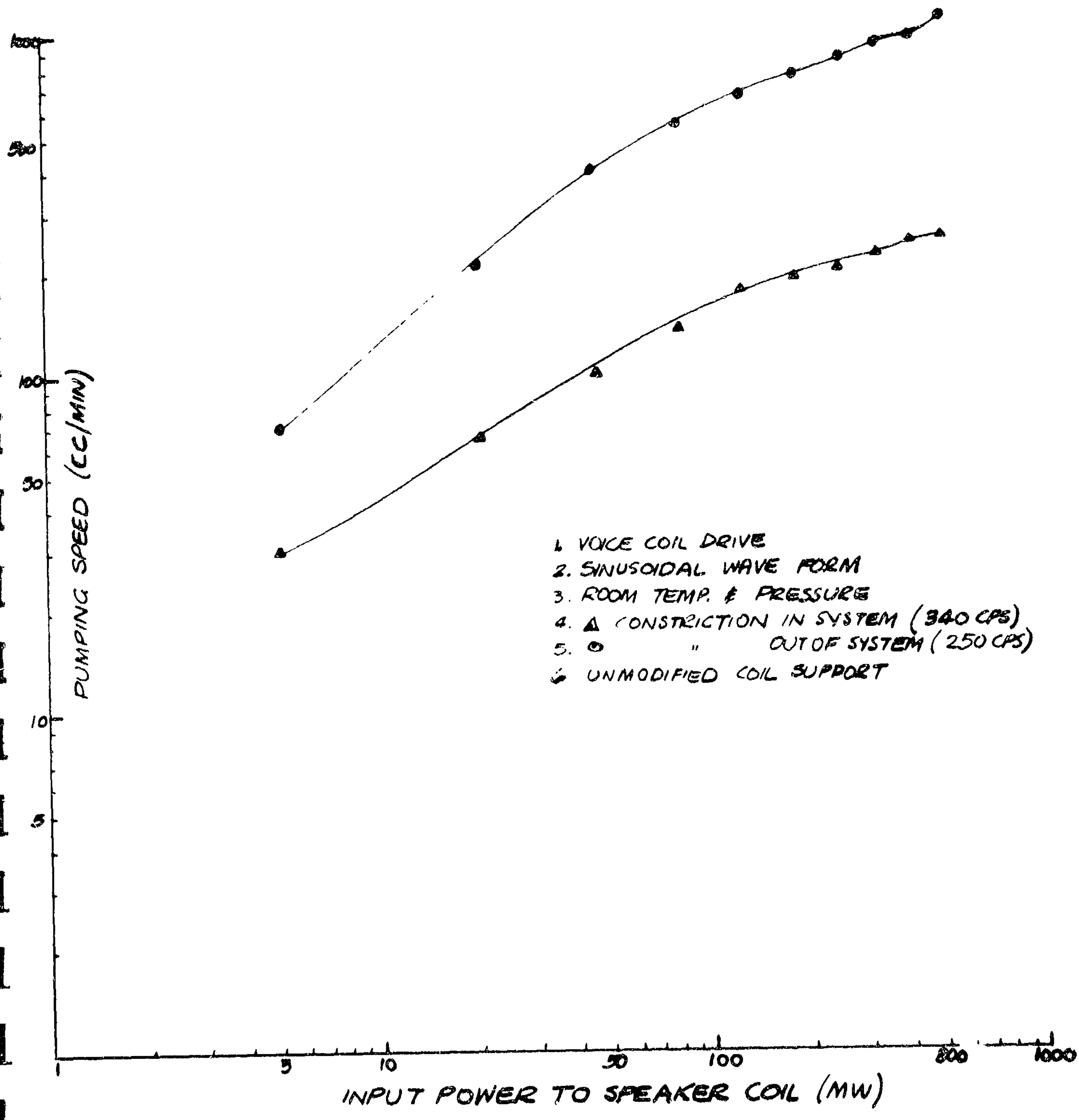

FIG 3.21 - PUMPING SPEED VS. INPUT POWER

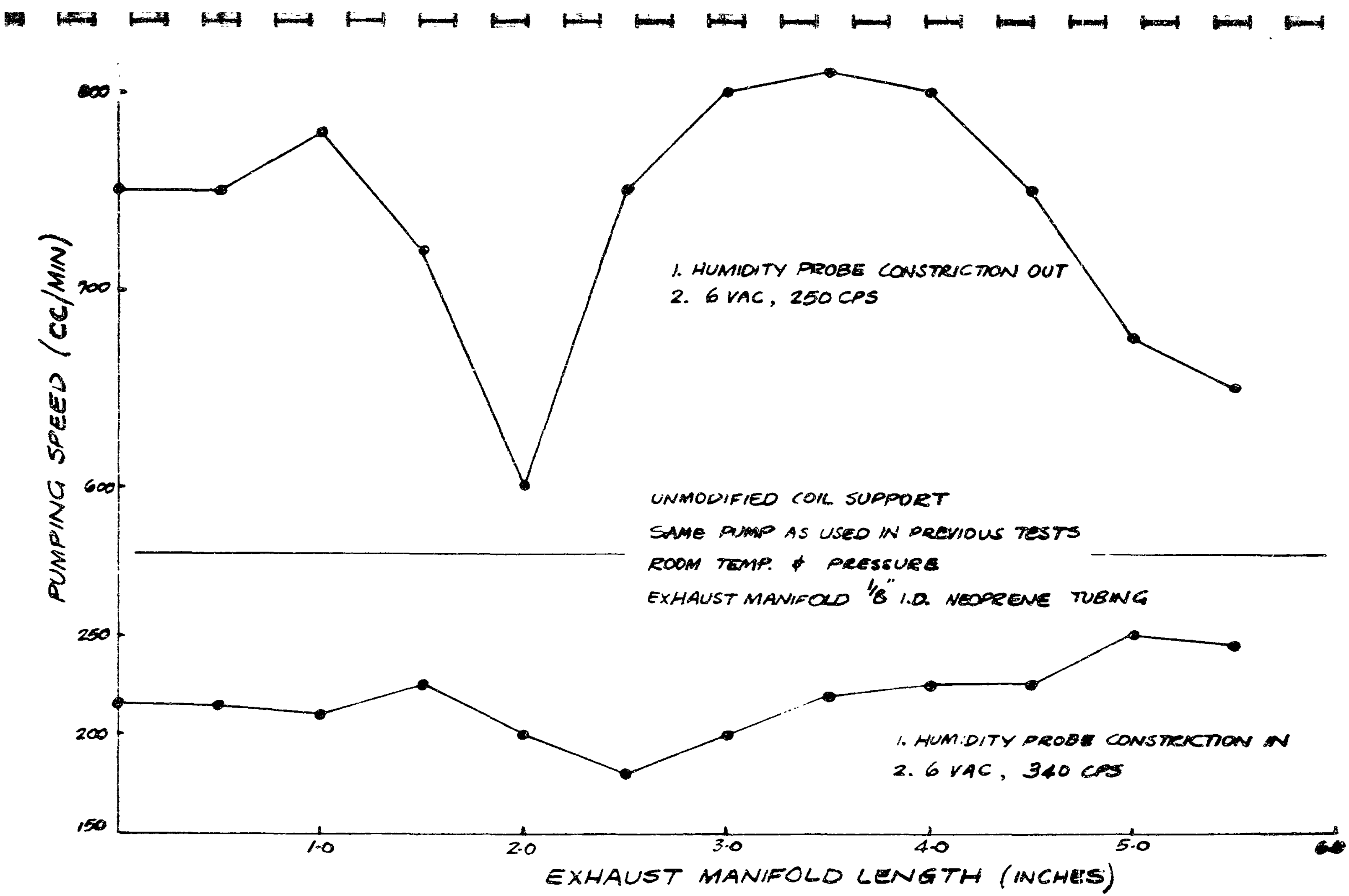

FIG 3.22 - PUMPING SPEED VS. EXHAUST MANIFOLD LENGTH

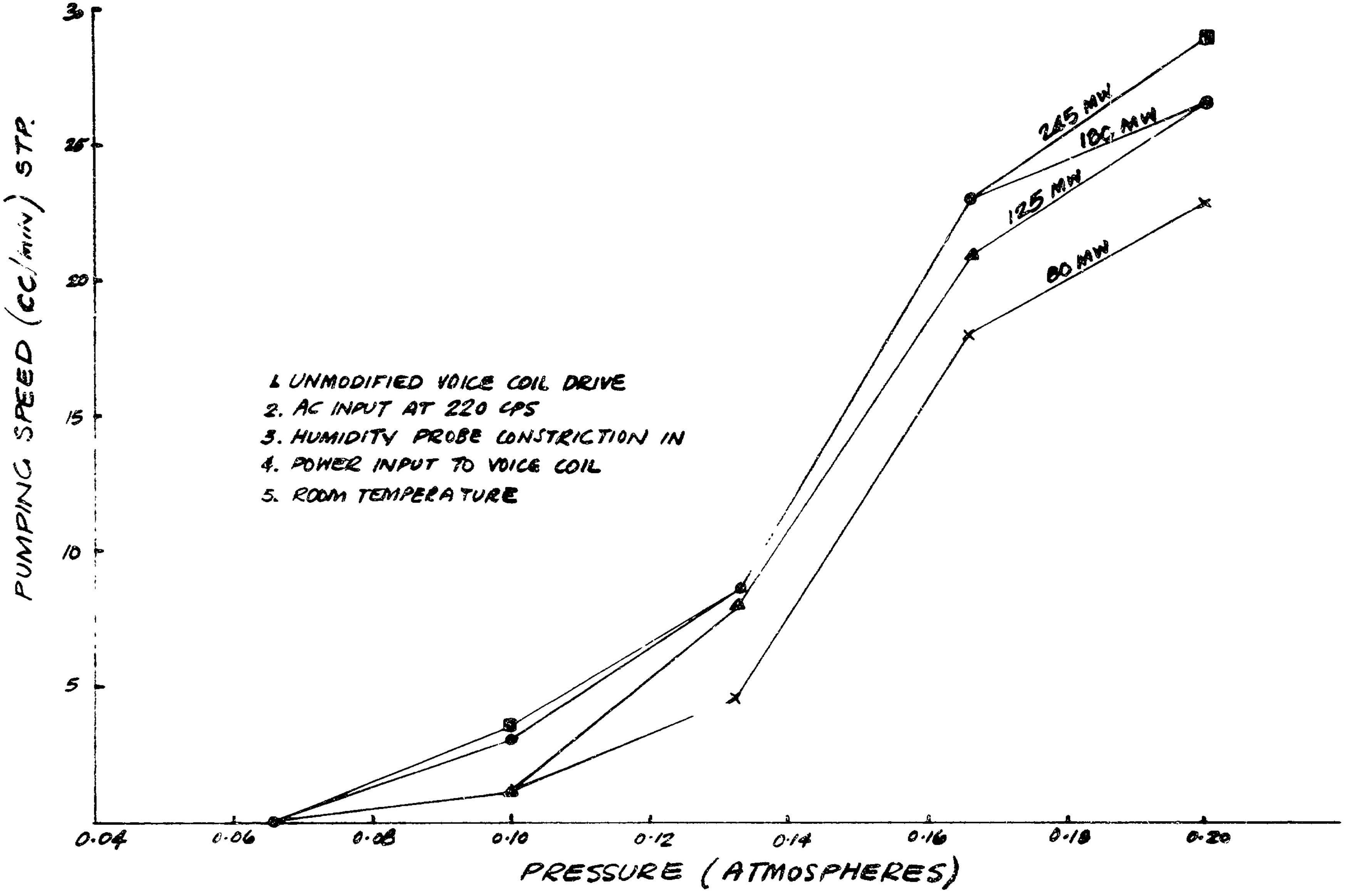

FIG 3.23 - PUMPING SPEED VS. PRESSURE AT VARIOUS POWER LEVELS

in performance without appreciable increase in size or weight. In summary, he stated that designing such a unit is a straightforward problem and would not require technological advances in either materials or design.

Summary:

A diaphragm pump of the type discussed in this report has experimentally demonstrated that it can move the required amount of air through a MRI model humidity probe constriction (a tube 0.015 in. I.D. by 2 1/2 in. long) and associated plumbing at low ambient pressures, e.g., 0.03 ATM. Detailed optimization of the pump at low ambient pressures and temperatures will provide pumping speeds of 1 - 2 cc/min at ambient pressures of 0.01 ATM. over an operating temperature range of 14°F to +158°F (-10°C to +70°C) with a power consumption of less than 250 mw. Such an optimized pump would be in the form of a disc approximately 2 1/2 in. O.D. by 3/8 in. thick and would weigh less than 1 1/2 oz.

Such a pump could be driven by an electric motor or a voice coil driver. Small efficient motors exist which can perform this task. It is necessary to investigate and then design a transmission and servo system which would allow control of the pumping speed while maintaining the motor at its peak operating efficiency. In addition, it would be necessary to select new motor component materials so that it would survive the sterilization environment as well as launch vehicle environment. Such a process consists of qualifying the existing design to meet mil specs which presents several engineering problems; however, such a task is well within the present state of the art and therefore does not present insurmountable difficulties. As stated previously, the voice coil driver is a straightforward engineering design problem that can be solved with existing techniques. The principal differences between these drivers centers around a balance of relative efficiency, environmental adaptability and reliability. A motor is fundamentally more efficient (40% or more vs a maximum voice coil efficiency of 25%); however, it is subject to bearing overload due to launch vibrations, possible bearing lubrication changes occurring during the months of space travel; performance change of commutator brushes due to launch environment and space travel, etc. Moving parts of the voice coil driver utilize flexural type supports and therefore are not subject to sliding or rolling frictional losses due to time or environment.

Further development work should be performed on both drivers before a selection can be made to give the optimum of the two drives for a particular space vehicle system. The tests and considerations discussed here show that either system can have the desired pumping performance (say 10 cc/min of STP air at pressure ranges between 0.1 and 0.01 atmospheres) at the required power and weight levels.

THE READOUT SYSTEM

It was decided that the readout system should indicate continuously and should adequately cover a range from about 1/6 ppm to 90 ppm while putting out 0 to 5 volts. When the cell reliability at moisture levels below ' ppm is better demonstrated, the readout system can be given appropriately more sensitivity.

Attention was given to readouttechniques which could partially overcome moisture sensor limitations, but these techniques seemed too complex to employ at this time when the sensor limits have not been completely determined. One method to minimize the unknown background leakage current was to integrate moisture in the sensor; this involved leaving the voltage off of the sensor for a period and then measuring the current pulse when the voltage was turned on again. Another method was to subtract out electronically any initial leakage current.

A nonlinear readout system has been provided in the breadboard model which puts out 0 to 5 volts D. C. for a moisture range considered representative. With solid state techniques it is a straightforward matter to treat the input current levels of the moisture cell, to provide whatever nonlinearity may be desired, and to handle any reasonable output impedance levels desired. Since the optimum input current range has not been determined, since the telemetering output impedance level has not been exactly specified, and since the data handling capability of the data transmission link has not been established, the final readout system could not be designed. The one provided demonstrates the feasibility of one approach.

Figure 4.1 shows the important features of the circuit: simply, the cell and a resistive element in series, across a 24-volt battery, with the output taken across the resistive element. The passive resistive element includes a network of resistors and diodes, as shown in Fig. 4.2 . The 100-ohm resistor serves as overload protection in case the moisture cell draws excessive current as it gets 'dried out' (presumably this is only a factor when the cell is tested or demonstrated at the high moisture contents on earth, not in operational use). The 6.8 V silicon Zener diode 1N3016 keeps the output voltage from getting unnecessarily large. The other resistors and silicon diodes provide the nonlinearity as shown in Fig. 4.3 . At a gas flow rate of 4.5 cc/min of STP air, the 'microamperes' abscissa can be interpreted as parts per million of water vapor. Because of the nonlinearity, the unit is more sensitive at low moisture values than at high moisture values. At low values, an output change of 0.1 volt corresponds to a variation of moisture level of 0.16 ppm; at high values, an output change of 0.1 volt corresponds to a variation of 3.7 ppm, 23 times less sensitivity. A data transmission accuracy of one part in 50, roughly six

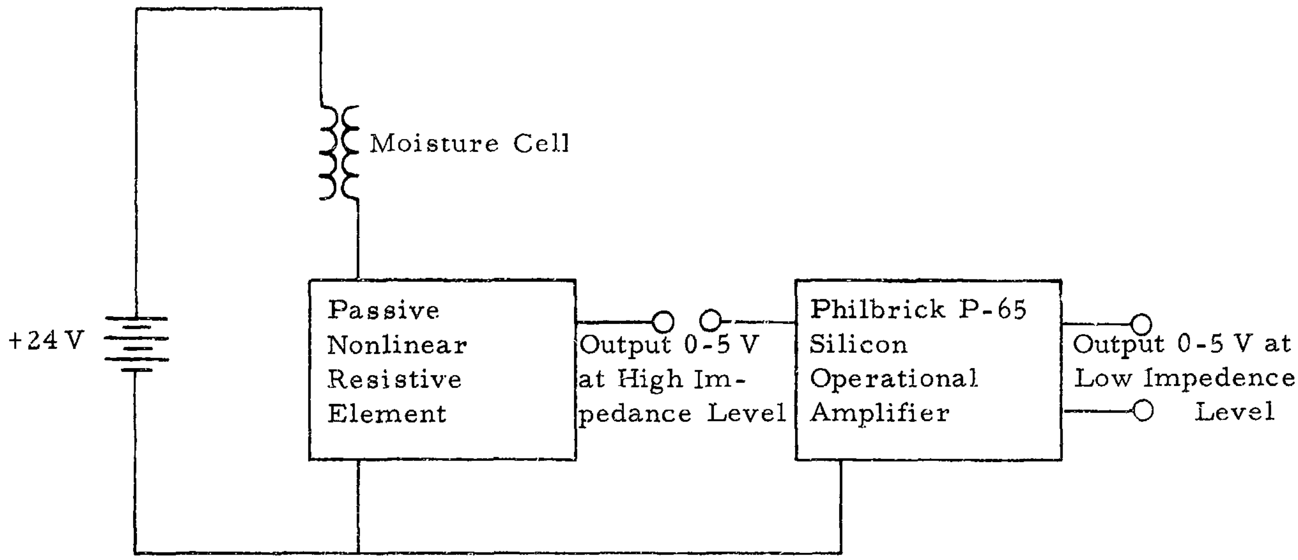

SIMPLIFIED SCHEMATIC OF MOISTURE SENSOR READOUT

Fig. 4.1

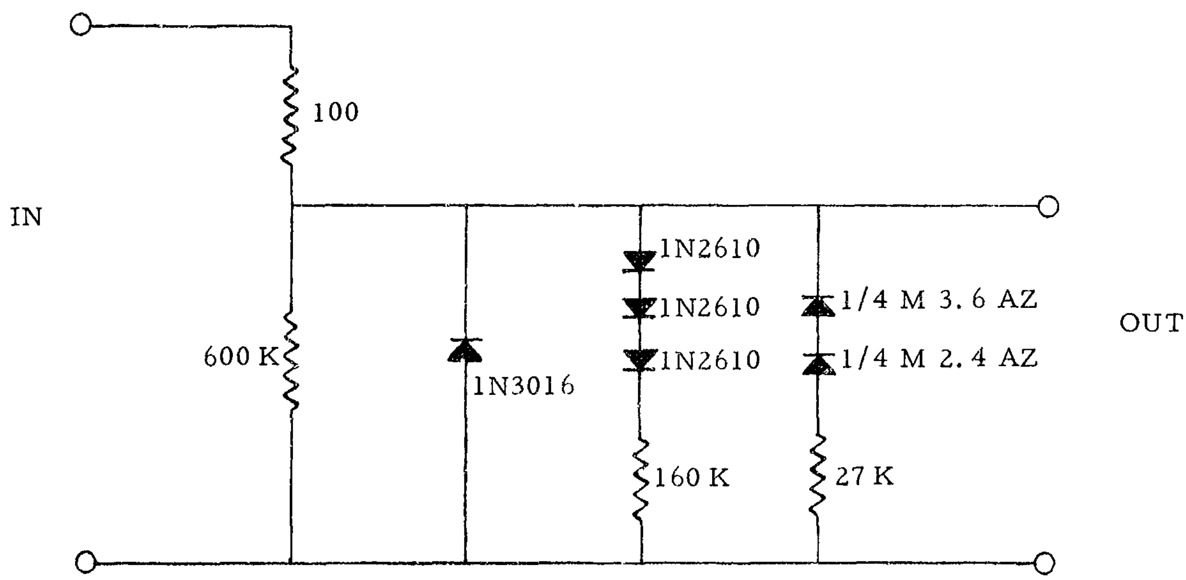

NONLINEAR PASSIVE RESISTIVE ELEMENT

Fig. 4.2

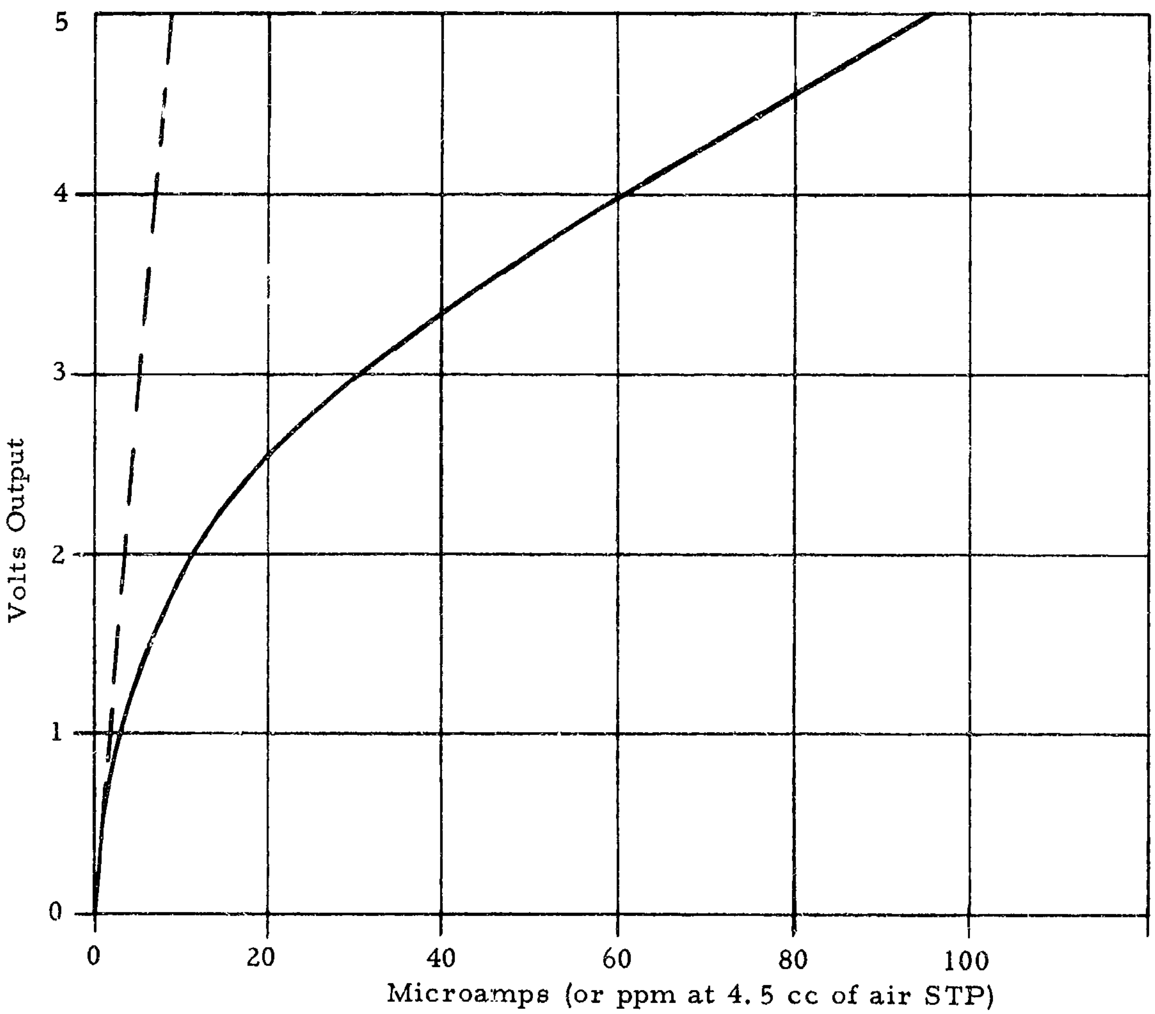

NONLINEAR OUTPUT CIRCUIT, WATER VAPOR METER

Fig. 4.3

bits of information, here covers levels from 0.16 to 97 ppm, about 2-1/2 decades.

The power consumption of the output circuit is negligible; at 100 microamperes, it is 2.4 milliwatts. If a lower output impedance is required, the Philbrick P-65 silicon amplifier as demonstrated shows that a lower impedance level can be obtained at low drift with practical size, weight, and power consumption. The P-65 here puts out 0 to 5 volts through 5000 ohms, while consuming about 70 milliwatts. Its weight, without case, is just a couple of ounces, and it is small. The P-65, which is not considered part of the breadboard, shows that the desired output level can be handled by simple, standard techniques. An 'ultimate' design could thus utilize comparable techniques, although probably some of the nonlinearity would be put into the feedback elements of the operational amplifier, and also even less power consumption can be provided. Such a design can readily go down two orders of magnitude in sensitivity level compared to the demonstrated unit if desired.

For demonstrations at typical earth atmosphere moisture levels, the sensor current will be on the order of 10 or 20 milliamps; for such cases it is convenient to put a 100-ohm resistor across the passive element output so that 5 volts output corresponds to 50 milliamps.

THE POWER SUPPLY

One of the goals of the program was to obtain an instrument which would operate with a total power requirement of no more than 500 mw. We believe the system designed is capable of being built to satisfy this specification, although the feasibility breadboard which was delivered requires more power than that.

The largest power requirement is for the pump drive electronics. These circuits were hurriedly assembled at the end of the program without being designed for optimum efficiency. As a result, they are using much more power than is necessary. For example, in the feasibility breadboard at maximum pumping rate there are 750 mw being supplied to the output transistors driving the output transformer in the voice coil pump drive. Only 180 mw is reaching the voice coil itself, partly because of mismatch of the output impedances. This poor efficiency can be greatly improved with a consequent power saving.

Although the goal of 500 mw can be met, there might be substantial advantages if more power were made available. The design of the pump is largely determined by the amount of power available. If more power were available a much larger volume of air could be pumped. This would have two important advantages; it would permit the operation of the instrument at higher altitudes above the Martian surface, and it would permit higher flow rates through the sensor, thus effectively increasing its sensitivity. It would also permit other pump designs to be considered, which might be less efficient but perhaps would be smaller in size.

The breadboard model operates from a dry battery power pack. Four DC voltages are required, +24, +6, -6, and +2.7. No special effort was made at this stage to eliminate the requirement of any of them. This is largely a problem of electronic circuit design, and it may well be that several of them could be eliminated in future circuits. It should be pointed out that in the figures given in this report on weights and powers, no consideration was given to possible weight or power requirements of circuit components which might be required if it were necessary to get these voltages from a single 26 VDC supply. However, this is not believed to be a serious problem, and considerable simplification is doubtless possible here.

THE FEASIBILITY BREADBOARD

GENERAL

The feasibility breadboard has been designed and constructed only to test and demonstrate feasibility of the system components. It has not been designed, for instance, to withstand sterilization temperatures. Attached to the central system package is a box containing the battery power supply. These units are shown in the photograph Fig. 6. D. The power supply provides +24, +6, -6, and +2.7 volts from dry batteries. In a later model efforts would be made to utilize the basic 24 volts available and thereby reduce the power and weight consumed by DC to DC converters.

The central system package consists of three decks or tiers. The bottom deck contains the nonlinear output circuitry and potentiometers for making various adjustments. The second, or middle, deck contains the system electronics; flow servo, heater servo, flow sensor bridge resistors, and pump oscillator. The top deck contains the pump, pump drive and flow sensor. Unless mounted elsewhere for a test, the moisture cell is mounted above the flow sensor.

The breadboard model can be mounted on a vacuum jar plate. Through this plate passes the required electrical leads with multiple pin connectors between the basic system unit and the power supply unit. The sensor output appears across the labeled terminals on the power supply box in the form of a non-linear voltage. The lower of the two toggle switches turns on the power for all components except the moisture cell. The upper switch controls the power for the moisture cell.

OPERATION

With the power switches in ON position the system will be operating. One minute should be allowed for the flow sensor to heat up to operating temperature. With the system operating, various adjustments can be made by adjusting the several potentiometers on the bottom deck. These controls will be discussed in order of left to right as you face the adjustment end of the row of potentiometers.

1. The leftmost potentiometer changes the balance of the flow sensor bridge circuit. The potentiometer is located electrically on the sensing thermistor side of the bridge. If an indication of the bridge balance is required, a 25 or 50 microamp meter with about 7000 ohms resistance may be placed across the two outside insulated leads from the flow sensor which are connected to pins on the top deck. When there is no air passing through the flow sensor then the bridge is not in balance. If this imbalance is to be checked, simply pull loose the air line between the pump and the flow sensor. Pinching this line is also possible, but care must be taken to see to it that all passage is blocked.

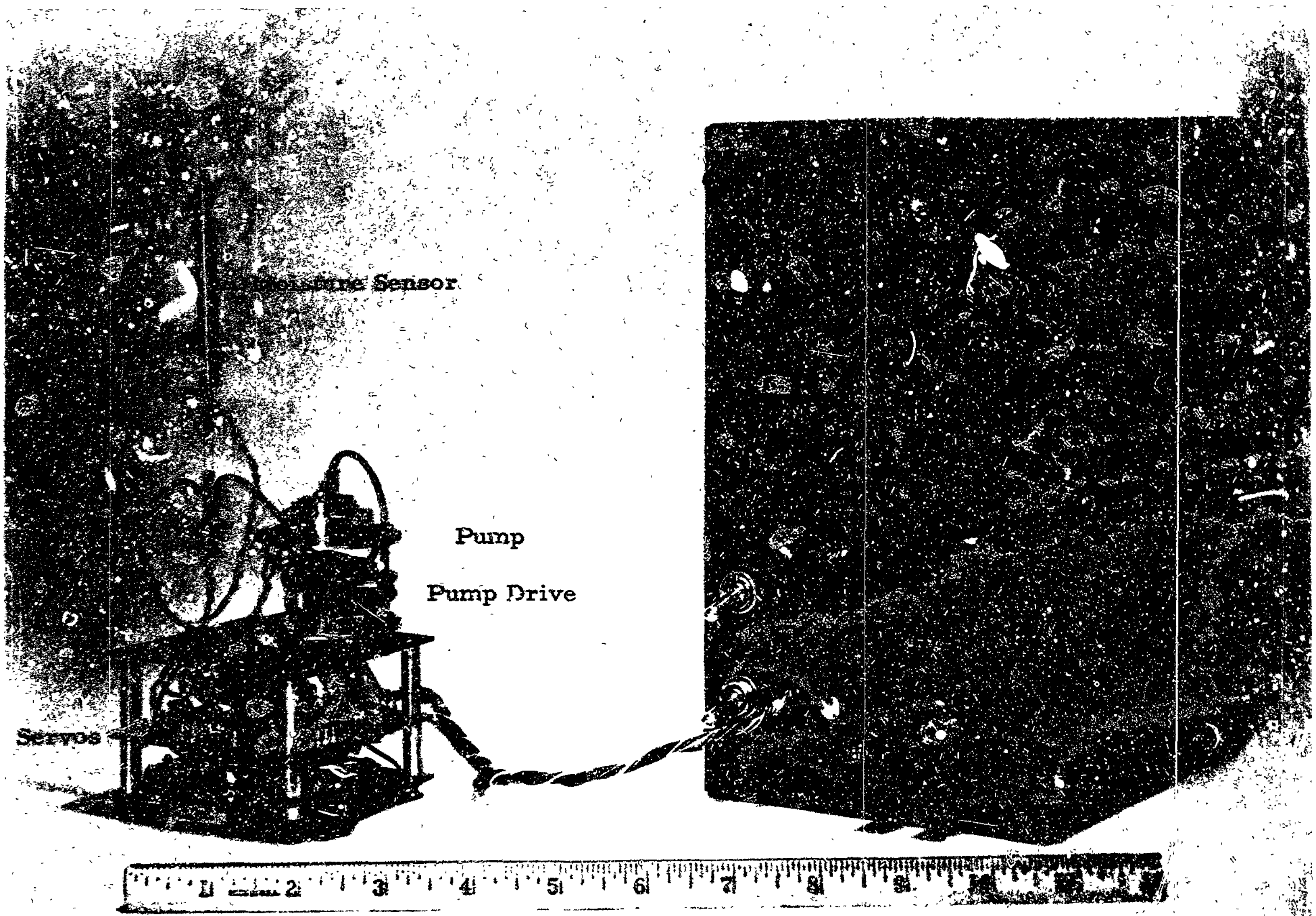

FIG. 6.0 - FEASABILITY BREADBOARD

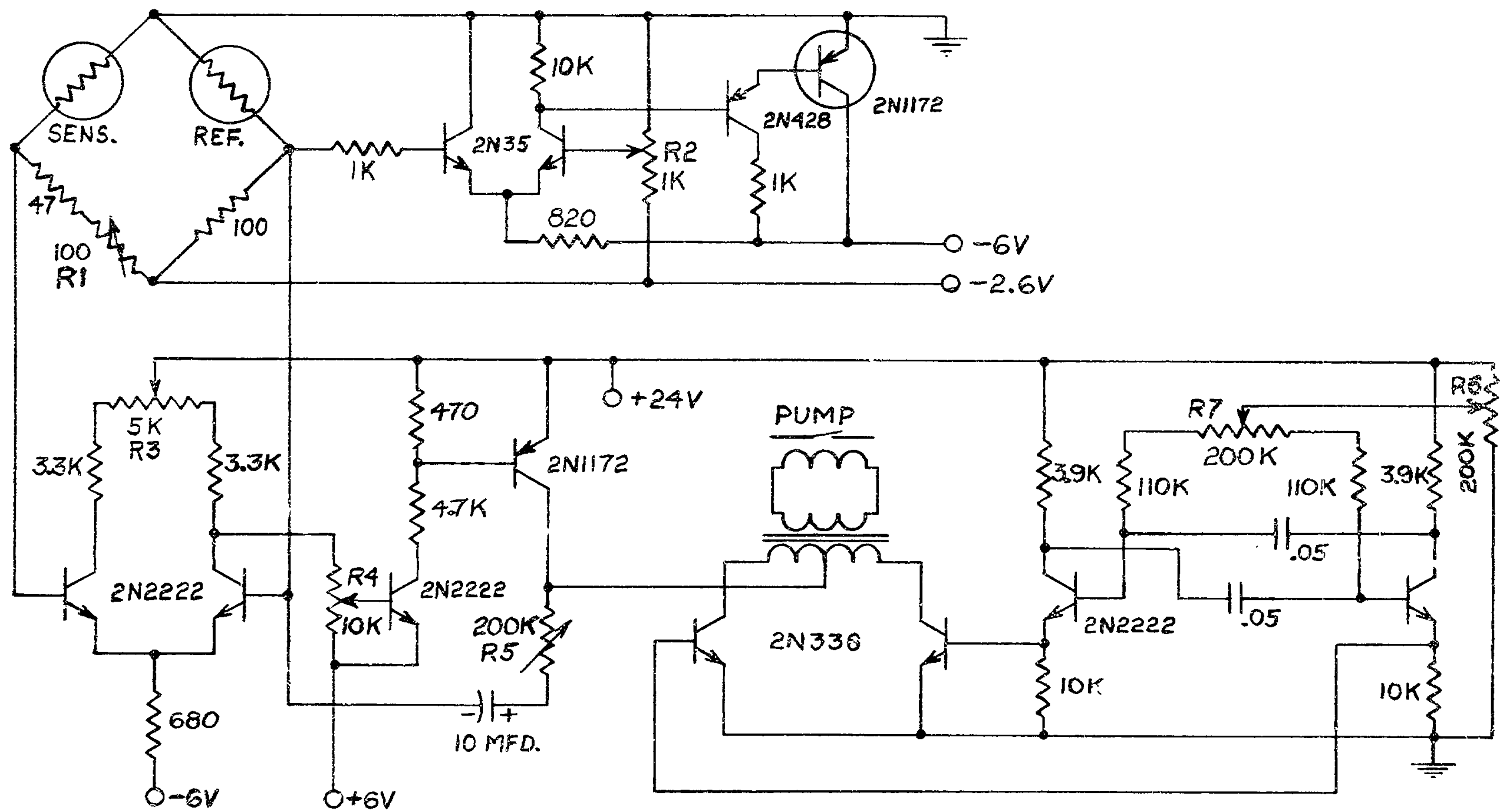

meteorology research, inc. altadena, calif. RESEARCH DESIGN INSTRUMENTATION		
SCALE: NONE	APPROVED BY:	DRAWN BY RJB
DATE: 9-5-62		REVISED
FEASIBILITY BREADBOARD CIRCUIT		
		DRAWING NUMBER

Fig. 6.2

Since the bridge is balanced when the system is operating, the flow rate at which the bridge is balanced may be increased by increasing the bridge imbalance when there is no flow. This is done by mounting an external flow meter in the system and increasing the pumping rate by turning the bridge potentiometer. Once set, the flow will remain constant and a meter reading of the bridge should show a continual zero.

A possible error that can be encountered is caused by the fact that the flow sensor can "see" an alternating airflow as well as a steady one way airflow. This can be caused, for instance, if the intake valve in the pump is not fully closing on the compression stroke. A simple check is to pinch off the air flow upstream of the flow sensor. If the pump does not go to full output and the bridge go to its imbalance position, then the flow sensor is seeing an alternating airflow.

2. The second from the left potentiometer controls the temperature of the flow sensor case. The flow sensor should operate somewhat warmer than the maximum expected ambient temperature. It is important to note that any readjustment of the temperature will require readjustment of the flow with the leftmost potentiometer.

Before turning the potentiometer, connect a 500 milliamp meter into the heater power circuit. Do this by disconnecting the yellow minus 6 volt lead in the power supply and placing the meter in series between the lead and the battery. With this meter connected you can see the effect made on the heater. When the flow sensor is cold, it will require a few seconds to heat and the current will be about 300 milliamps. Once the operating temperature has been reached the current will drop down to a few tens of milliamps. The current will, of course, depend on the thermal insulation of the flow sensor. If the temperature is to be reduced, turn the potentiometer screw counterclockwise. Allow the sensor to cool (holding it between your moist fingers will speed the process) until the current comes up again and see if this is the desired temperature. Repeat until the desired setting is reached. To raise the temperature simply turn up the heat a quarter turn, wait until the current comes down and check, and repeat if necessary. The process of bringing heat up instead of down is quicker.

3. The third potentiometer controls the balance of the servo amplifier. It should be adjusted so that the system operates with the flow bridge close to zero. Naturally any adjustment of this control requires a meter across the flow bridge as described in the paragraph about the bridge balance potentiometer. It is not necessary that the bridge be exactly on zero as long as the amplifier balance does not change while in operation.

4. This potentiometer in the center controls the pump servo amplifier gain. Normally the system will operate with gain at a maximum.

Occasionally, however, it may be desirable to reduce the gain for such studies as servo stability.

5. This potentiometer, third from the right, is part of the negative feedback loop in the servo amplifier. It should be adjusted to obtain servo stability in the operating range desired.

6. The potentiometer second from the right controls the frequency of the pump oscillator. It should not be adjusted without the aid of an oscilloscope as the wave symmetry will be affected.

7. The far right potentiometer controls the symmetry of the wave form of the signal to the pump. When the frequency is adjusted the signal may no longer be properly symmetrical. With an oscilloscope the wave form may easily be corrected with this control.

Moisture Cell:

Supplied with the moisture cell is a short piece of stainless steel tubing with a tube fitting attached. This tubing may be inserted carefully into the receiving end of the moisture cell so that it may be attached to dry air producing apparatus. The output of the moisture cell is discussed in Section 1, but as a general rule it may be stated that the electrical current through the cell is 1 microamp per milligram per kilogram for every 4.5 cc of air flow per minute.

Test Suggestions:

The breadboard feasibility model has been designed and constructed only to demonstrate the feasibility of the system in meeting the requirements of the task of measuring moisture in the atmosphere of Mars. Such problems as temperature and weight, which can obviously be met by standard techniques, have not necessarily been met in this breadboard model. Some tests, however, may be made to demonstrate nonstandard abilities. These abilities lie chiefly in the characteristics of the moisture cell and the pump including the servo system. Some of these tests are enumerated below:

<u>Moisture Cell</u>

1. Temperature

Operate the moisture sensor to see that it works properly over the desired range of ambient temperature.

2. Moisture Indication

There are two ways to introduce a gas carrying moisture to the cell. First, using the tube fitting supplied, simply connect a pressure supply to the cell at a known rate and take the measurements. The other, and preferable system is to have a relatively large tube carry the gas past the sensor and let the pump system draw the correct amount into the cell. This latter method has the great advantage of avoiding a huge moisture gradient across the cell casing. The major difficulty will be obtaining the proper known dryness of the carrier gas. Section 1 of this report discusses this problem at considerable length.

Care must be taken not to have a change in temperature cause a change in water vapor in the carrier gas. If a cold bath technique is employed, wholly denatured alcohol is a good bath liquid and can be cooled to temperatures yielding moisture contents of a few parts per billion. Only stainless steel has been found to be satisfactory for conducting the gas and even that is not as good as is desired.

Pumping System

A most important test is measuring pumping capacity against decreasing pressures. A pellet flow gauge of sufficient capacity may be used to check the correctness of flow. A gauge going to about 1000 cc per minute should be used. Run the pump, decrease the pressures and check the pellet gauge. A correction factor for ambient pressure will be required to calculate the resulting mass flows. Watch out for acoustic resonance effects in the gas lines which may radically affect pumping rates.

Power Consumption

The simplest test would seem to be to measure the current out of the various batteries to obtain wattages. In the case of the flow heater, the power will be decreased if the sensor is embedded in a thermal insulator.

SYSTEMS CONSIDERATIONS

This section contains some general discussions of problems relating to adapting the MRI moisture instrument to installation in the space vehicle instrumentation package.

Size:

While the breadboard constructed to demonstrate the feasibility of the development is smaller than the specified goal of 500 cc, it would be possible to reduce the size even more with routine engineering improvements if this were found to be desirable. Without the use of molecular electronics, the servo circuits could be reduced to half their present volume. The biggest item that would be difficult to reduce is the pump, but some shrinkage is possible. It would seem that a volume of 150 to 200 cc would be relatively easy to attain.

Weight:

Like volume, the weight of the feasibility breadboard was well under the goal of one pound. Perhaps the 11 ounce breadboard weight could be reduced by 20%, but beyond this would be quite difficult.

Installation:

Considerable flexibility in the installation and mounting of the parts of the moisture instrument is possible. For example, the servo amplifiers and readout electronics can be located remotely from the other parts. The moisture sensor should be located so that it connects to a duct to the outside in such a way as to minimize wall effects in the duct. The very dry duct walls will absorb moisture and cause an erroneous reading if this precaution is not taken. This problem would exist for any type of sensor and must be considered in the design of the instrument capsule. The flowmeter and the pump can be separated from the moisture sensor if this is necessary. However, since the pump would be designed to work most efficiently with a particular plumbing arrangement, this must be known in advance, if possible. The pump exhaust must be connected to a static source on the capsule so that the pump will operate properly. The inlet to the moisture sensor must also be in a position which will not experience positive pressure beyond that provided by the pump, since the pump is not a valve and cannot shut off excessive flow. The location of these inlets can be determined by the application of ordinary aerodynamic computations, however.

Power:

As pointed out in a previous section, the operation of the instrument would be improved if more power were made available. The unit is designed to operate off DC power, but if other sources were available they could be used with some slightly higher weights. The instrument electronic design needs to be integrated with the exact power source available at an early stage of the development if maximumsimplicity and economy of power are to be achieved.

Alternate System:

If some other variables were known from computations or measurements, it would be possible to build an extremely simple system. For example if the rate of descent were known, the moisture sensor could be connected so that the flow of gas through it would be caused by the falling of the instrument capsule through the Martian atmosphere. This would eliminate the flowmeter, its servo, and the pump and its servo. Power, weight and number of parts would be reduced by 80% to 90%. Such a device is so simple that it might well be considered in any case as a back-up for the regular moisture instrument.

RECOMMENDED FUTURE WORK

Since the work described in this report, and the feasibility breadboard delivered, indicate that all the major requirements for a moisture measuring device for the Martian atmosphere can be met or exceeded by the MRI device, consideration should be given to the further steps necessary to provide such a device for an actual Martian probe. This might well consist of two major steps; first an engineering program which would result in the delivery of an engineering prototype, and second, the design and production of the final models for the space vehicle. The first of these steps will be discussed in the following paragraphs.

GENERAL

We should first define what we mean by an engineering prototype. This would be an operating model of the instrument which in size, weight, configuration and performance would be as identical to a final model as it would be possible to specify at the time of its construction. It would be capable of operating under all the expected environmental conditions, including sterilization, and would subsequently be tested under these conditions. The main likely difference between it and the final model for installation on the actual vehicle would be in its mechanical lay-out. The exact location and size of ducts in the overall Martian instrument package will have some effect on the performance of the moisture meter, and while the moisture meter can be adapted to a wide variety of such lay-outs, it is supposed that these might not be finally specified at the time this engineering prototype would be under construction.

The engineering prototype would be the result of an engineering development program based on improvements made on the feasibility breadboard already delivered. Most of these improvements could be carried out rather rapidly, if necessary, by parallel engineering efforts on the several components of the MRI moisture system. It should be pointed out, however, that because of the difficulties described in Section 1 relating to setting up and operating a test and calibration system at these very low moisture levels, there would of necessity be a good many months of testing required to prove-in the operation of the sensor and the whole system at the lowest moisture levels. The drying out process just cannot be reliably hurried, and the time which must elapse between readings can be days in many instances. It should be noted that this is a characteristic of tests of <u>any</u> moisture sensor operating at these low levels, and is not a characteristic of the MRI device. Our experience has indicated that any process which seems to speed up this procedure must have the most critical scrutiny to make sure that spurious effects are not inadvertently introduced.

The program which MRI would pursue in this engineering development is discussed in outline below, broken down by system components.

CALIBRATION METHODS

The difficulties encountered with moisture sinks and sources in the standard gas supply would be further investigated. The effect of coatings, platings or mechanical modification of the inner walls of the stainless tubing would be investigated, and other materials would also be tested. Possible elimination of wall effects by various combinations of duct size and aerodynamic variations in flow patterns would be explored. The possible elimination of the long time delays when changing moisture levels in a single set of tubing would be investigated by trying multiple sources of different moisture levels to see if these can be switched or valved to the sensor under test without introducing extraneous effects. At present we know of no better control of moisture level than cold traps, but if other schemes are possible they would be tried. This work on calibration methods would be the most time consuming part of the engineering investigation.

SENSOR

While we believe that the present form of the sensor will be adequate, some additional work should be done on the effect of P_2O_5 coating thickness and the method of applying the coating. Possible increasing of the speed and efficiency of the chemical reaction by operating the sensor at an elevated temperature would also be investigated. The effect on the time constant and sensitivity of various parameters such as size, length and flow rate through the sensor would also be tested. Much of this work would depend upon the successful production of the standard moisture source at these levels, so this would of necessity be performed in the later stages of the calibration investigation discussed in the preceding paragraph. The final design of a satisfactory sensor seems reasonably well assured, however.

FLOWMETER

If power were a critical item, and sufficient time and money were available, work might be done on the AC heated and temperature compensated flowmeter. The present unit works satisfactorily, however, and if power supply considerations were held the same, or relaxed somewhat, no great amount of work on the flowmeter would be necessary.

PUMPING SYSTEM

This would be a two-pronged attack on the diaphragm pump and its drive unit. The first step would be to optimize the diaphragm pump for the particular pumping speed, constrictions, plumbing, pressure, temperature, etc. that would be encountered. Measurement of the characteristics of this pump would then allow the design of a driver to meet these particular characteristics.

The initial work would then consist of attaching a force transducer to the push-pull rod activating the diaphragm of a test pump designed from information supplied by this report, and proceeding with an optimization program to provide the desired pump speed at the desired pressure and temperature. This would consist of obtaining families of curves relating push-pull forces, displacements, and time with various diaphragm-washer and piston relationships, flapper valve, pump chambers, intake and exhaust manifold size and shape, etc. Such a program would produce a maximum efficiency pump with known input requirement, e.g. power, force, displacement, frequency, pumping speed, control characteristics, resonance effects, etc. A drive system could then be designed to meet these particular requirements. A dual approach utilizing existing non-mil spec electric motors and a specially designed voice coil driver would then be instigated to determine relative performance and efficiency. If both driver systems survived this program, then a detailed reliability study program would be made to select the system which had the greatest reliability when integrated into the instrument package. Particular attention would be given to the problems of acoustic resonance in the piping of the final system, since this has a marked effect on the overall operation of the pump. Advantage would be taken of resonance effects whenever possible.

READOUT CIRCUITS

Presumably the telemetering impedance and other characteristics would be defined by this time by JPL and the final design of the non-linear output circuits could be made to conform with these requirements. This is not considered to be other than a straightforward electronic circuit exercise, and so no great difficulty or time is expected to be required.

POWER SUPPLY

It is assumed that by this time the final power supply characteristics for the vehicle instrument package will be known, and the moisture meter will be tailored to fit these requirements. Here again, this is expected to be a routine electronic engineering job. It should be pointed out, however, that if more power were available for the moisture unit, for example one watt instead of 1/2 watt, the operation and reliability of the unit would be greatly improved. This should be known as early as possible, however, in order to reap the maximum benefit in the engineering design.

SERVOS

The two electronic servo amplifiers and the pump oscillator would be redesigned to incorporate silicon transistors and other high temperature components to withstand the expected environment. The circuits would also be mechanically redesigned in to a more or less final configuration for the final operational model. This is not expected to be a major task.

SYSTEM INTEGRATION

Throughout the engineering development work contemplated in this further program, consideration would be given to the integration of the moisture meter instrument in the final overall instrument package. The extent to which this could be effectively done would be dependent upon how well frozen is the final system package at this stage. The MRI moisture instrument is quite flexible in this regard, but advantage should be taken of all systems specifications as they become known, to minimize last minute design changes in the final model to be installed in the space vehicle.

POSSIBLE MINIMUM SYSTEM

In Section 7 a possible simplified system was mentioned which would need neither flow sensor or pump. It would depend upon the descent of the instrument package to provide the air flow. If the air speed during descent were computed, and the viscosity estimated, the flow through a moisture sensor on the instrument package could be computed. If other parameters such as temperature and pressure are measured or can be inferred, an alternate arrangement would be to have a flask or air tank open to the outside air through the moisture sensing cell. As the instrument capsule descended the air would flow through the sensor into the tank as in a standard rate-of-climb instrument. This also would permit a continuous moisture measurement without flowmeter, servo, or pump. An instrument designed using either of the above techniques would be very simple and reliable and might weigh as little as two or three ounces and require only 25 or 50 milliwatts of power. It should certainly have serious consideration as a back-up for any other moisture measuring instrument.

TIME SCHEDULE

All of the above work could be carried out in a six-month period, if the projects were performed in parallel, except for the development of the calibration and test technique. We believe this will require a minimum of eight months, although with additional support to permit some parallel effort here, this might be compressed somewhat if necessary to meet a particular shooting schedule lead-time. A ten to twelve month program at a lower level of effort might produce better results than a more hurried and equally expensive six to eight month program, since it would give more time for thorough tests on the calibration system.

We would be glad to discuss further details of this proposed program with the JPL staff at any time. We feel that the work performed so far by MRI on this project indicates that the further investigation leading to an engineering prototype of this moisture meter would be very worth while.

TABULATION OF RESULTS

Item	Demonstrated In Best Experiment	Feasibility Breadboard	Projected After 6-8 Month Eng. Development	"Ultimate" After 2-3 Year Development
MOISTURE SENSOR Threshold in PPM	3	3	0.5	0.01
FLOWMETER Minimum Operating Pressure in Atmospheres	0.01	0.01	0.01	0.01
PUMP (Motor driven) Flow Rate in cc/min	0.8		4.5	
At Ambient Pressure in Atmospheres	0.03		0.05	
PUMP (Voice Coil driven) Flow Rate in cc/min	3	5	4.5	
At Ambient Pressure in Atmospheres	0.1	0.5	0.05	
POWER REQUIREMENTS				
Flowmeter Bridge	80	80	80	
Flowmeter Heater	120	120	10	
Pump & Servo Drive	910	910	400	
WEIGHT (Ounces)	11	11	8	4
DIMENSIONS (Inches)	3 x 3 x 3	3 x 3 x 3	2 x 2 x 2	d = 3 h = 1 (Cylinder)